2003-09

Cost benefit analysis of adjustable speed drives aboard Arleigh Burke class destroyers

Weekes, Godfrey D.

Monterey, California. Naval Postgraduate School

NAVAL
POSTGRADUATE
SCHOOL

MONTEREY, CALIFORNIA

THESIS

COST BENEFIT ANALYSIS OF ADJUSTABLE SPEED DRIVES ABOARD ARLEIGH BURKE CLASS DESTROYERS

By

Godfrey D. Weekes

September 2003

Thesis Advisor:	Robert W. Ashton
Co-Advisor:	John Ciezki
Second Reader:	Andrew A. Parker

THIS PAGE INTENTIONALLY LEFT BLANK

REPORT DOCUMENTATION PAGE			Form Approved OMB No. 0704-0188
Public reporting burden for this collection of information is estimated to average 1 hour per response, including the time for reviewing instruction, searching existing data sources, gathering and maintaining the data needed, and completing and reviewing the collection of information. Send comments regarding this burden estimate or any other aspect of this collection of information, including suggestions for reducing this burden, to Washington Headquarters Services, Directorate for Information Operations and Reports, 1215 Jefferson Davis Highway, Suite 1204, Arlington, VA 22202-4302, and to the Office of Management and Budget, Paperwork Reduction Project (0704-0188) Washington DC 20503.			
1. AGENCY USE ONLY *(Leave blank)*	**2. REPORT DATE** September 2003	**3. REPORT TYPE AND DATES COVERED** Master's Thesis	
4. TITLE AND SUBTITLE: Cost Benefit Analysis of Adjustable Speed Drives Aboard Arleigh Burke Class Destroyers			**5. FUNDING NUMBERS**
6. AUTHOR(S) Godfrey Weekes			
7. PERFORMING ORGANIZATION NAME(S) AND ADDRESS(ES) Naval Postgraduate School Monterey, CA 93943-5000			**8. PERFORMING ORGANIZATION REPORT NUMBER**
9. SPONSORING /MONITORING AGENCY NAME(S) AND ADDRESS(ES) N/A			**10. SPONSORING/MONITORING AGENCY REPORT NUMBER**
11. SUPPLEMENTARY NOTES The views expressed in this thesis are those of the author and do not reflect the official policy or position of the Department of Defense or the U.S. Government.			
12a. DISTRIBUTION / AVAILABILITY STATEMENT Approved for public release; distribution is unlimited			**12b. DISTRIBUTION CODE**

13. ABSTRACT ***(maximum 200 words)***

As the U.S. Navy seeks new and innovative ways to maximize its return from a finite budget, an evaluation of its operational practices must be done. Electrical power consumption and fuel efficiency are major factors in the Total Operating Cost (TOC) of naval ships and systems. An evaluation of an alternative mean for delivering electrical power to motors and pumps was conducted with the understanding that principles of the findings could be applied to fans as well. Adjustable Speed Drives (ASD), AC induction motors, AC synchronous motors, centrifugal pumps, and positive displacement pumps were examined. The technical challenges associated with ASDs were explored. MATLAB was used to calculate the potential power savings to be gained by introducing ASD technology to the Firemain and Chilled Water Systems. MATLAB was also used to calculate fuel cost savings from reduced consumption of Shipboard power.

14. SUBJECT TERMS Adjustable Speed Drive, Pulsewidth Modulation, Affinity Laws, AC Induction Motor, Insulated Gate Bipolar Transistor			**15. NUMBER OF PAGES** 93
			16. PRICE CODE
17. SECURITY CLASSIFICATION OF REPORT Unclassified	**18. SECURITY CLASSIFICATION OF THIS PAGE** Unclassified	**19. SECURITY CLASSIFICATION OF ABSTRACT** Unclassified	**20. LIMITATION OF ABSTRACT** UL

NSN 7540-01-280-5500 Standard Form 298 (Rev. 2-89)
Prescribed by ANSI Std. 239-18

THIS PAGE INTENTIONALLY LEFT BLANK

Approved for public release; distribution is unlimited

COST BENEFIT ANALYSIS OF ADJUSTABLE SPEED DRIVES ABOARD ARLEIGH BURKE CLASS DESTROYERS

Godfrey D. Weekes
Lieutenant, United States Navy
B.S., Savannah State University, 1995

Submitted in partial fulfillment of the
requirements for the degree of

MASTER OF SCIENCE IN ELECTRICAL ENGINEERING

from the

NAVAL POSTGRADUATE SCHOOL
September 2003

Author: Godfrey D. Weekes

Approved by: Robert W. Ashton
Thesis Advisor

John Ciezki
Co-Advisor

Andrew A. Parker
Second Reader

John P. Powers
Chairman, Department of Electrical and Computer Engineering

THIS PAGE INTENTIONALLY LEFT BLANK

ABSTRACT

As the U.S. Navy seeks new and innovative ways to maximize its return from a finite budget, an evaluation of its operational practices must be done. Electrical power consumption and fuel efficiency are major factors in the Total Operating Cost (TOC) of naval ships and systems. An evaluation of an alternative mean for delivering electrical power to motors and pumps was conducted with the understanding that principles of the findings could be applied to fans as well. Adjustable Speed Drives (ASD), AC induction motors, AC synchronous motors, centrifugal pumps, and positive displacement pumps were examined. The technical challenges associated with ASDs were explored. MATLAB was used to calculate the potential power savings to be gained by introducing ASD technology to the firemain and chilled water systems. MATLAB was also used to calculate fuel cost savings from reduced consumption of Shipboard power.

THIS PAGE INTENTIONALLY LEFT BLANK

TABLE OF CONTENTS

LIST OF FIGURES

LIST OF TABLES

THIS PAGE INTENTIONALLY LEFT BLANK

ACKNOWLEDGMENTS

I would like express my deepest gratitude to Prof. John Ciezki, Prof. Robert Ashton, and Mr. Parker for their patience and guidance throughout this project. I would like to thank my love, Debra, and all my family and friends who gave me strength and encouragement during my time at NPS.

THIS PAGE INTENTIONALLY LEFT BLANK

EXECUTIVE SUMMARY

The US Navy must operate within the boundaries of a congressionally approved budget. In order to maximize the return on its operations, the navy is exploring innovative ideas such as crew swaps and contracted ship painting. The U.S. Navy has already decided that a ship with an Integrated Power System (IPS) would benefit from savings in manpower, efficiency, maintenance, and fuel. This study sought to quantify the potential fuel cost savings from the implementation of Adjustable Speed Drives (ASD) aboard an Arleigh Burke destroyer.

The use of ASDs in the commercial marine environment has long been touted as a means to improve efficiency while reducing the cost of operations. ASDs control motor speed so that it finely corresponds to varying load requirements. The result is increased energy efficiency, improved power factor, and process precision. ASDs afford other performance benefits such as soft starting and overspeed capability. They also can eliminate the need for expensive and energy–wasting throttling mechanisms such as control valves and outlet dampers.

ASDs must comply with several military standards before installation aboard naval vessels can be considered. Military standards typically go beyond the quality assurance standards of private industry. This is in anticipation of the unique environment in which the devices will have to operate. The military standards cover issues from Total Harmonic Distortion (THD) to vibration tolerances.

Conventional control of a flow system through a throttling device is inefficient. ASDs afford the opportunity to change the flow of the system by decreasing or increasing the speed of the motor. Different ASD control strategies can ensure that the device operates at an optimal efficiency point. The result is a power savings, which leads to fuel cost savings.

The firemain and chilled water system were chosen for study and analysis in this thesis. The current mechanical throttle control of the systems leads to power waste. A 230 gpm differential between the flow the firemain needs to provide and the actual flow through the system. This 230 gpm difference is the result of the pressure control valve

dumping the excess flow in order to maintain proper system pressure. An ASD would minimize or eliminate this loss of power. A MATLAB program was created which utilized the systems operational parameters and the affinity formulas to determine the potential power savings yielded by an ASD. The affinity formulas govern the relationship between the speed of the pump, the flow in the system, the head pressure, and the needed brake horsepower. The simulation only considers the implementation of an ASD on a fire pump and a chilled water pump. The analysis demonstrated a potential 38% reduction of input power required for the two pumps.

Using the results from the MATLAB power analysis, another MATLAB program was created to determine fuel savings. A fuel cost savings in excess of $12,000 or 1% over a two year period was realized. Table E1 illustrates the fuel cost savings. Table E2 lists potential pump/motors that could benefit from ASD installations

	Fuel (gallons)	**Cost**	**Days Underway**	**Total fuel cost**	**Fuel Savings**
Underway (Deployed)	2944	$1.29	138	$524,247	
Underway (Deployed w/ ASD)	2913	$1.29	138	$518,572	$5674
Underway (Not-Deployed)	2944	$1.29	162	$615,237	
Underway (Not-Deployed w/ASD)	2913	$1.29	162	$608,758	$6479

Table E1: Fuel cost savings over 24 a month training and deployment cycle.

.

Unit	Quantity	Motor Rating
Fire Pump	6	150 hp
Centralized Sea Water Cooling Pump	5	50 hp
Chilled Water Pump	4	250 hp
Hydraulic Oil Power Module Pump/Motor	2	100 hp
SSGTG Sea Water Cooling Pump	3	10 hp
VCHT Pump	8	7.5 hp
Lube oil Service Pump	4	60 hp
Potable water Service pump	2	10 hp
Total	34	

Table E2: Potential pump/motors applications for ASDs.

THIS PAGE INTENTIONALLY LEFT BLANK

I. INTRODUCTION

A. PURPOSE

Finite budgets force the U.S. Navy to continuously seek new cost saving measures to meet its obligation to defend the nation. The Navy has pursued innovative ideas to meet these goals. Contracting out jobs normally done by sailors such as painting and food services, experimenting with rotating whole ships' crews on deployment, and reducing the ships' crew size are but a few of the cost saving initiatives that are being pursued by the navy. The U.S. Navy has decided that a ship with an Integrated Power System (IPS) would realize savings in manpower, efficiency, maintenance, and fuel. Whether a conventional electrical system or an IPS, both may benefit from the addition of Adjustable Speed Drives (ASD) for motor control. This thesis examines the feasibility of placing ASDs aboard DDG-51, Arleigh Burke class destroyers. The related research question is to formulate an analysis strategy and quantify the operational cost savings

B. ADJUSTABLE SPEED DRIVE BACKGROUND

The technology to control the operation of an Alternating Current (AC) motor continues to develop at a fast pace. ASDs are a significant part of this development where it is used to provide continuous range process speed control vice discrete speed control. Currently the most promising ASD technology use Insulated Gate Bipolar Transistors (IGBT) to generate the variable voltage and frequency required to control the speed of an AC motor via Pulse Width Modulation (PWM) microprocessor-based algorithms.

1. Advantages of an ASD

An ASD is capable of adjusting both speed and torque of an AC motor. The primary purpose of an adjustable speed drive is to control an AC motor so it operates at its optimal speed for the task. In considering ASDs, overall system efficiency improvements vary significantly depending on the application. Shipboard systems could potentially benefit greatly from the addition of ASDs, since a majority of the equipment onboard a ship operates for extended periods of time, only partially loaded. ASDs also provide for

soft starting of equipment in which a motor must accelerate from standstill. This reduces the mechanical stress on both the motor and equipment driven by the motor. By reducing in–rush current ASDs also reduce system voltage sag that can occur when a large motor starts. Voltage sags can dim lights and cause other equipment to shut down or restart [2]. Other ASD advantages include:

- more low speed torque for applications where nominal motor torque is required close to zero speed,
- quieter motor operation which reduces audible and transmitted noise, and
- improved low speed stability which minimizes low speed oscillations.

2. Disadvantages of an ASD

There are disadvantages associated with the adoption of ASDs. These disadvantages must be weighed when deciding whether or not to make an investment in ASD technology. Initial cost is often the primary obstacle to ASD implementation. However, the potential energy savings payback and process control enhancement with ASDs may justify the investment. Payback is generally not significant if the average throttled speed requirement of a given application is low, between 90%-100%. In the commercial world as a general rule, a 2 1/2-year projected maximum payback period validates the purchase of an ASD [3].

ASDs are complex solid–state electronic devices, necessitating more technical training for the maintenance personnel. ASD manufacturers have significantly improved the diagnostic capabilities of their products, but they still require properly trained personnel to maintain them. Also, ASDs are more susceptible to hostile environmental conditions, such as dust and temperature changes [3].

Another intrinsic problem is that ASD motors can produce more heat than a conventional single–speed machine. In particular at low speed and for a constant torque load, the machine losses are approximately constant but with less natural convection. If the motor produces a high level of heat while operating at low speed, overheating may result. [3]

The National Electrical Manufacturers Association (NEMA) established standards for electrical motors. One such standard is for a fully–loaded motor with Class B insula-

tion running at 50% rated speed on a constant torque load should not overheat. If the motor is run below 50% speed continuously, it will most likely overheat. A motor with Class F insulation and fully loaded should be able to have its speed decreased by approximately 20% speed without overheating. The lower the continuous operating speed below the motor overheating point, the more the motor and drive must be derated. [3]

The output waveform generated by the ASD is a non-linear waveform. This waveform creates harmonics in the system. The harmonics depend on the switching frequency and the modulation strategy. Less complex strategies, such as six–step operation, can lead to significant current harmonics that in-turn create additional heat in the motor. Normally, ASDs create between 5-8% more heating in a motor when compared to that same motor running on a pure sinusoidal waveform from the power line. [3]

ASDs are installed between the power supply and the motor. Installing an ASD will naturally decrease system reliability, as now there are two pieces of equipment that can fail rather than just one. The robust nature of IGBT-based power converters and the maturation of the technology lead to a high reliability for these drives. ASD manufacturers have published Mean Time Between Failure (MTBF) values of 4-14 years compared to the MBTF of 3-4 years for pumps. Elements of an ASD are illustrated in Figure 1. Only after examining the pros and cons of installing ASDs aboard the destroyers can a determination be made whether it is an investment the navy should make.

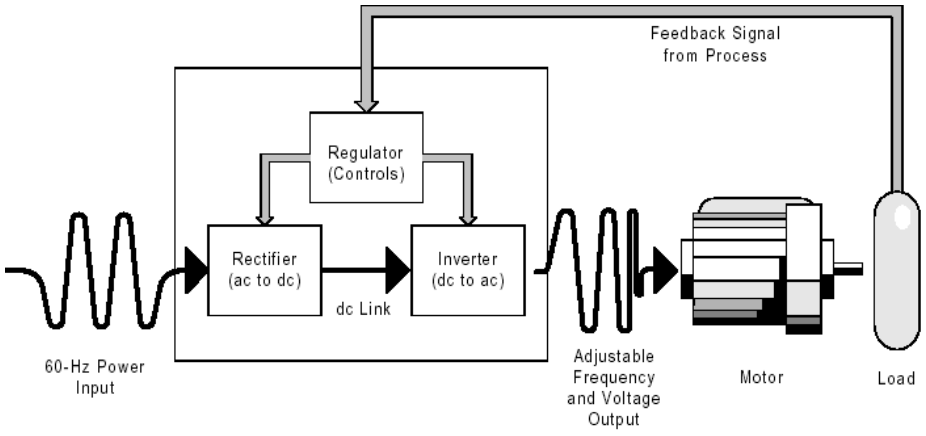

Figure 1. Elements of an ASD [From Ref. 1.].

C. PROLIFERATION OF ADJUSTABLE SPEED DRIVES IN INDUSTRY

There are several examples of the use of ASDs in industry that support the theory that ASDs provide significant savings on the operational cost of equipment in private industries.

For example, a university laboratory complex had a hot water circulation system with both a 5-hp and a 30-hp pump. Pressure and flow were controlled by pressure reducing valves at the discharges of the pumps. After a feasibility study, an ASD was applied to the 30-hp pump to eliminate the use of valves. The factors that made this an attractive ASD installation included: high number of hours of operation, wide variation between maximum and minimum demands, and the elimination of throttling valves. The payback period, without utility incentives, was about four years. [2]

As the cost of electric power continues to increase, ASDs are becoming more popular in the car wash industry. The industry has found that adding ASDs is a reliable and cost-effective option for the electric motors within the facility. Adding ASDs to a car wash dryer system can often provide a return on investment within 14 months in electrical energy savings. A recent study completed at a car wash in the northeast United States concluded that the dryers were operating at idle with no car under them for more than 50% of the time. The installation of ASDs on dryer systems will reduce the total fan electricity consumption and demand, especially during standby or idle times. An independent study documented that operating the dryers at 90% of their rated capacity while actually drying a car and then dropping the speed to 50% while waiting for a car to move down the conveyor would reduce the electric power consumed by over 50%. [5]

D. CURRENT U.S. NAVY EFFORTS: BATH IRON WORKS REPORT

The U.S. Navy recently commissioned a study for the evaluation of available Commercial Off-The-Shelf (COTS) ASD equipment, the identification of ASD applications on the Arleigh Burke Class DDG platform, and the evaluation of ASD control systems' architecture and logic. The study assessed the viability of the integration of ASDs for shipboard applications. The potential fuel cost savings achieved by the operation of pumps and fans at reduced speeds were calculated. It considered potential life cycle cost

savings in implementing ASDs on an IPS with a zonal electrical distribution system as well as a conventional AC power distribution system. [4]

When assessing the COTS ASD systems several factors must be addressed before their implementation aboard U.S. Navy vessels. One of the most critical issues is their ability to withstand vibration and shock encountered aboard a warship. [4]

In implementing ASDs aboard Arleigh Burke destroyers, the potential noise reduction of the platform is quite significant. The reductions will come from underwater and airborne radiated noise sources. The reductions in underwater noise will be a result of reducing the noise radiated by pumps, motors, and fluid flowing through the piping system. The reductions in airborne noise will be a result of reducing Heating Ventilation, and Air Conditioning (HVAC) and cooling fan air velocity generated noise. [4]

E. THESIS OVERVIEW

Chapter I introduced the concept of ASDs and has enumerated various benefits associated with their implementation. The disadvantages or problems facing those seeking to implement the use of ASDs were highlighted. Two industrial examples were presented while more can be found in the references [1–5]. A U.S. Navy-sanctioned study into ASDs was introduced.

The fans and centrifugal pumps installed in shipboard HVAC and other fluid flow systems are typically driven by single–speed motors operating digitally (on or off). ASDs offer a method of supplying the required flow without the use of throttling valves. This means that ASDs would eliminate the costs associated with installation and maintenance of throttling devices, and reduce the power consumption of flow systems. ASDs potentially offer substantial life cycle cost savings opportunities on naval vessels.

Chapter II provides an overview of the elements of an ASD. The theory of operation of an AC induction motor, AC synchronous motor, voltage source inverter, and six types of harmonic filters are discussed. Chapter III examines the technical challenges associated with ASDs. Chapter IV explains the theory of operation of pumps and conventional methods of controlling flow in a pump system. Chapter V demonstrates the

potential power and fuel savings that can be achieved with ASDs. Chapter VI presents conclusions and recommendations for addendum to this work.

II. ELEMENTS OF AN ADJUSTABLE SPEED DRIVE

A. INTRODUCTION

An ASD is comprised of several elements: the motor, the inverter, the filter, and the control method. Basic theory behind the operation of these elements is explained in this chapter. Chapter II also provides a snapshot of some ASDs that are currently available from manufacturers and the potential number of fans and pumps on which the U.S. Navy could implement this technology. The chapter ends with the military standards that will govern the operational parameters of the ASDs.

B. MOTORS

1. AC Induction Motor

Nicola Tesla invented the AC induction motor in 1888. Figure 2 illustrates an early example [6].

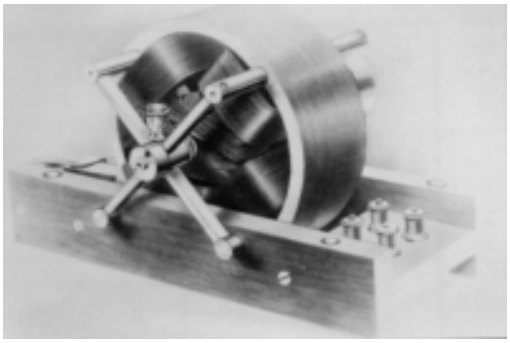

Figure 2. Tesla Two-Phase Induction Motor [From Ref. 6.].

Today, more than 90% of all motors used in industry worldwide are AC induction motors. They are the preferred choice due to their low cost and rugged construction [7]. The simple and rugged construction of the induction motor contributes to its reliability and makes it attractive for shipboard applications.

The name "induction motor" comes from the AC "induced" into the rotor via the rotating magnetic flux produced by the stator. The stator is the stationary part of an AC

machine. A simple three–phase stator is constructed by using three separate coils of wire with coil distributions spaced 120° apart. The stator structure is composed of metal (i.e., steel or aluminum) laminations with formed slots used to hold copper conductors. These primary windings are connected to a three–phase voltage source. The stator winding currents produce a rotating magnetic field that induces ElectroMotive Forces (EMF) in the rotor cage winding [8]. The induced EMF causes current flow and Magneto–Motive Forces (MMF) in the rotor. In turn, the rotor's MMFs produce a magnetic flux pattern, which also rotates in the air gap at the same speed as the stator-winding field [9]. Figure 3 shows the coils of the stator for an AC induction motor.

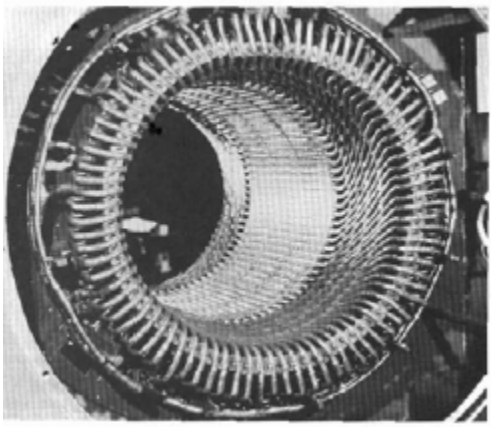

Figure 3. An AC Motor Stator with Preformed Stator Coils [From Ref. 10.].

The rotor is made of laminations over a metal shaft core. Radial slots around the periphery of the laminations house rotor bars with copper conductors shorted at the ends and positioned parallel to the shaft. The arrangement of the rotor bars leads to this machine being referred to as the Squirrel–Cage Induction Motor, shown below in Figure 4.

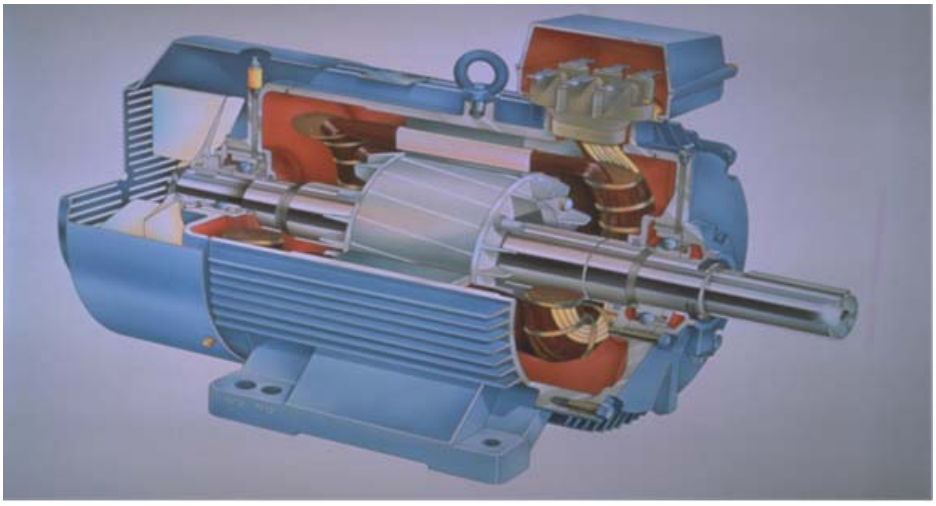

Figure 4. Squirrel Cage Induction Motor [From Ref. 7.].

Motor torque, τ , developed from the interaction of currents flowing in the rotor's bars producing the rotor magnetic field, $\vec{B}_r$, and the stator's rotating magnetic field, $\vec{B}_s$. The torque induced by the two magnetic fields is

$$\vec{\tau} = k\vec{B}_r \times \vec{B}_s, \tag{2.1}$$

where k is a constant that depends on the system of units used to express $\vec{B}_r$ and $\vec{B}_s$ [10]. The rotor can then be accelerated to a speed at which the electromagnetic torque is balanced by the load torque [9]. When the load torque balances the electromagnetic torque, the motor's speed becomes constant.

An induction motor rotor speed always lags the rotating magnetic field's speed, causing the rotor's bars to cut magnetic lines of force to produce torque. This speed difference is called slip. Slip is necessary to produce torque in a Squirrel–Cage Induction Motor. As the rotor and the magnetic field rotate at different speeds, the rotor cuts the lines of flux created by the stator thereby inducing voltage in the rotor. Slip is load dependent; therefore as the load increases or decreases, so does the slip. Slip, s , can be determined by the following formula [7]:

$$s = \frac{n_s - n}{n_s}, \tag{2.2}$$

where n_s is the speed of rotation of the magnetic field (or synchronous speed) in rpm and n is the rotor speed of the motor in rpm. The steady–state magnetic field rotation speed is dictated by

$$n_s = \frac{129 \cdot f_e}{P}, \tag{2.3}$$

in which f_e is the excitation frequency (in Hz) and P is the number of poles in the motor.

2. Induction Motor Losses

There are several aspects of power losses to the motor that must be taken into account in order to determine the motor's efficiency, η. The I^2R, heat losses, suffered by the stator, P_{SCL}, and rotor, P_{RCL}, windings are the most notable. Most shipboard applications call for the induction motor to operate with the smallest value of slip possible. This is due to the fact that motor's slip and rotor copper losses are proportional [10], as demonstrated by

$$P_{RCL} = sP_{AG}, \tag{2.4}$$

where P_{AG} is the power transmitted across the air gap. Hysteresis and eddy current iron losses account for the remaining power lost in the stator. The combination is called core losses, P_{CORE}. Other losses in the machine include friction and windage losses, P_F and P_W, and stray magnetic losses, P_{ML} [9]. The output power, P_{OUT}, is found by subtracting the machine's losses from the input power, P_{IN},

$$P_{OUT} = P_{IN} - (P_{SCL} + P_{RCL} + P_{CORE} + P_W + P_F + P_{ML}). \tag{2.5}$$

The motor efficiency can now be calculated,

$$\eta = \frac{P_{OUT}}{P_{IN}} \times 100\%. \tag{2.6}$$

3. AC Synchronous Motor

Synchronous motors are used in conjunction with ASDs in some larger capacity or high efficiency applications. They can be found in load-proportional capacity–modulated heat pumps, large fans, and large compressors [8]. They are more expensive than AC induction motors. The current process of procuring platforms and systems may make the purchase of synchronous motors an impractical decision.

A synchronous motor rotates at a constant speed, which is synchronous with the rotation of the magnetic field. The rotor magnetic field is established by either permanent magnets or by a field winding excited by a Direct Current (DC). Figure 5 illustrates the synchronous motor rotor structure. Synchronous motors are highly efficient motors. They are also more expensive than induction motors.

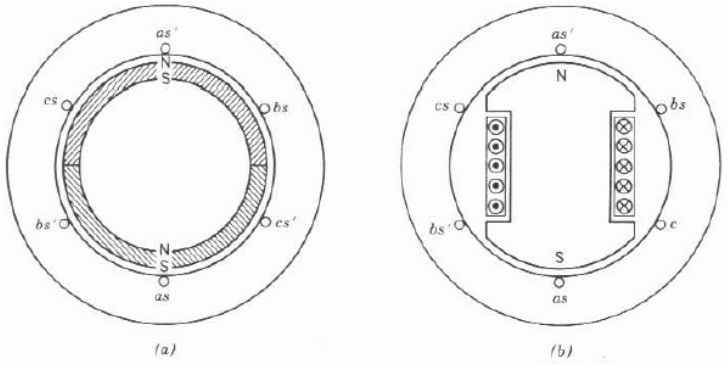

Figure 5. Structure of Synchronous Motors: (a) Permanent-Magnet Rotor (Two-Pole); (b) Salient-Pole Wound Motor (Two-Pole) [From Ref. 8.].

In large horsepower ratings, a wound-field construction is used while permanent magnets are typically used for small horsepower applications [7]. For synchronous motors, direct on-line started induction motor rotors are included so that they start like induction motors. These bars also provide a stabilizing influence during normal operation. The motor should be unloaded when started because the starting torque provided by the rotor bars is usually much less than full rated power. Starting the motor in this manner protects the DC coils wound around the rotor electromagnets. If this were not done, these coils would encounter very large voltage spikes during starting. For synchronous motors started with a power electronic converter, the frequency of the converter is automatically adjusted to "drag" the rotor up to the desired steady–state speed. A cutaway view of a synchronous motor is shown in Figure 6.

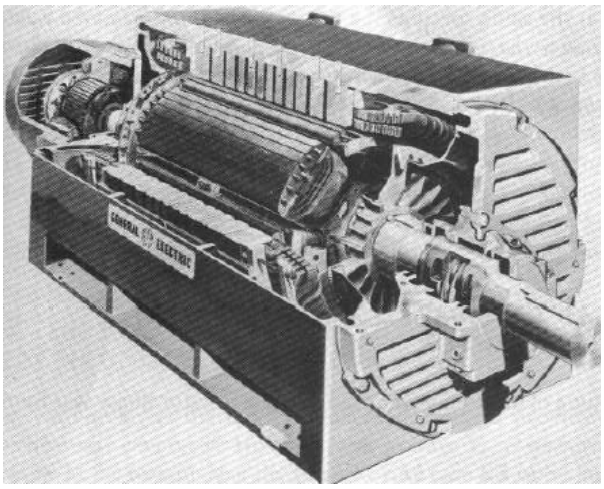

Figure 6. Cutaway View of a Synchronous Motor [From Ref. 10].

C. INVERTER

Inversion is the process of converting DC to AC. The inverter creates the variable frequency from the DC source that is used to drive an induction motor at a variable speed. There are two basic types of inverters, the Voltage Source Inverter (VSI) and the Current Source Inverter (CSI). VSIs are more common. A VSI creates a relatively well–defined switched voltage waveform at the motor's terminals. A strong DC bus voltage is maintained via a large capacitor in the DC link. The resulting motor current is then primarily governed by the motor load and speed.

VSIs are normally broken down into two forms, the Six-Step inverter and the PWM inverter. PWM inverters offer the best performance characteristics for ASD applications. The PWM inverter maintains a nearly constant DC link while combining voltage and frequency control within the inverter. A diode rectifier or battery provides the nearly constant DC link voltage. In general, modulation techniques fall into two classes, those that operate at a fixed switching ratio to the fundamental switching frequency also called block or "picket fence" modulation and those in which the switching ratio is continuously changing, usually sinusoidally, known as sinusoidal PWM [11].

The CSI provides a switched current waveform to the motor's terminals and uses a large inductor in the DC link to maintain a strong DC link current. Here the voltage waveform is primarily governed by the motor load and speed [11]. CSIs are typically used for high horsepower applications where waveform quality is not essential.

1. Insulated Gate Bipolar Transistor

IGBT technology is what makes the PWM so attractive today as a means of ASD motor control. IGBTs have a vertical semiconductor structure as shown in Figure 7 below. The physical layout is comparable to that of the vertical–diffused Metal Oxide Semiconductor Field Effect Transistor (MOSFET) with the exception of the presence of a p+ layer that forms the drain of the IGBT. Figure 8 and Figure 9 show the cross section view and schematic symbol for the IGBT, respectively.

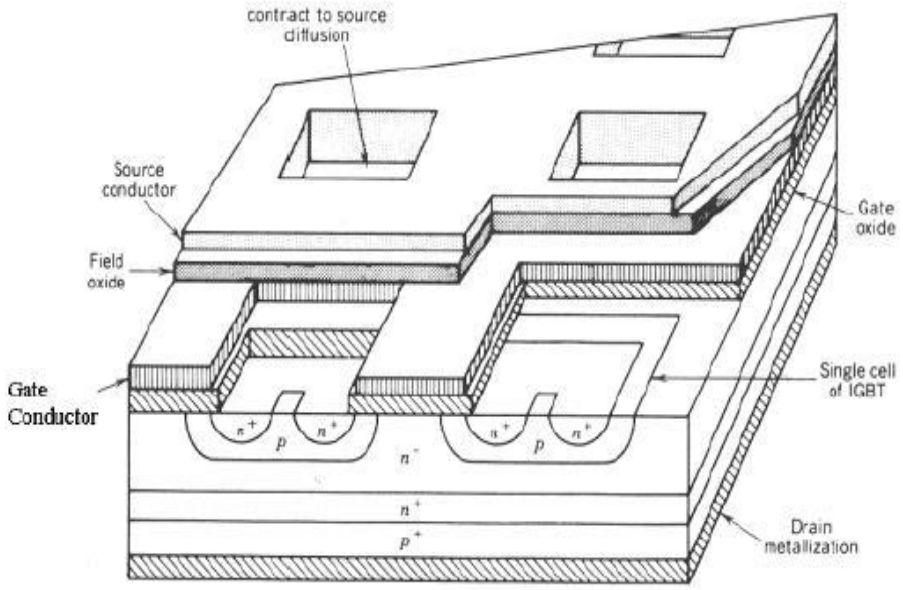

Figure 7. Perspective View of an IGBT [From Ref. 8.].

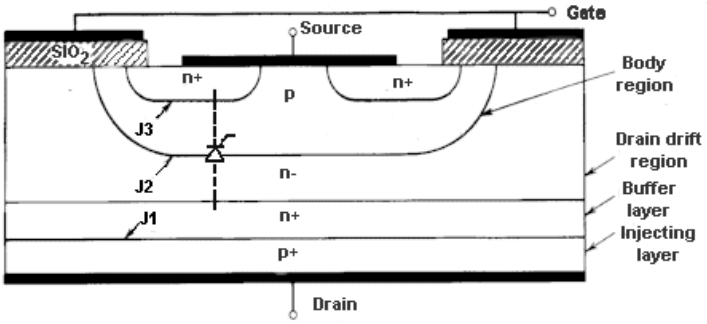

Figure 8. Cross-Section View of an IGBT [After Ref. 8].

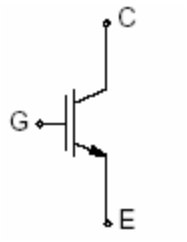

Figure 9. N-Channel IGBT Schematic Symbol [From Ref. 8].

The IGBT is a Bipolar Junction Transistor (BJT) that is designed to operate like a MOSFET. It has an injection region on its drain side to provide for conductivity modulation of the drain–drift region so that on-state losses are reduced. The IGBT is faster than a BJT but slower than a MOSFET. It has much smaller on-state losses than a MOSFET, equivalent to those of a BJT. The IGBT has high blocking voltage capabilities in addition to fast switching speeds. The turn-on speed of the IGBT is controlled by the rate of change of the gate source voltage. Figure 10 shows the current–voltage characteristics of a n-channel IGBT which closely resembles the characteristics of a logic level BJT except that the gate–source voltage, V_{GS}, is the control mechanism vice the input current for a BJT. The i_D-v_{GS} curve shown in Figure 11 below is identical to the transfer curve of the power MOSFET. The IGBT remains in the off-state while the v_{GS} is less than the gate threshold voltage, $V_{GS(th)}$ [8].

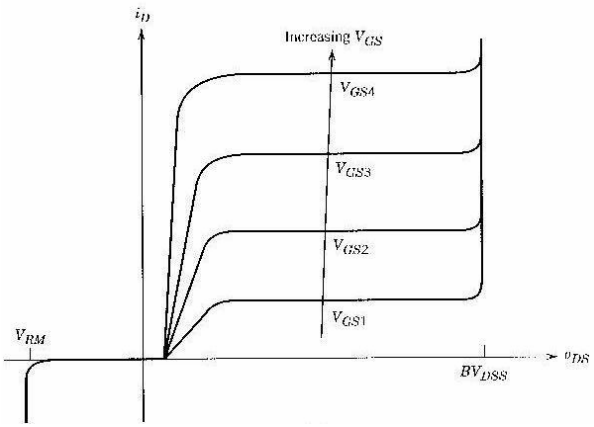

Figure 10. The IGBT I-V Characteristics [From Ref. 8.].

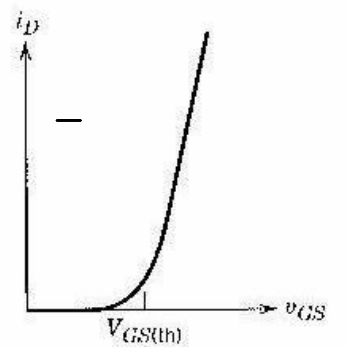

Figure 11. IGBT Transfer Characteristics [From Ref. 8].

It must be noted that the IGBT physical layout allows for the formation of a parasitc thyristor, shown in Figure 8, which if allowed to turn on (also known as "latch-up") would negate "gate control" of the IGBT. The IGBT would be destroyed because of power dissipation produced by excessive collector-to-emitter current. Both the manufacturer and the user must take steps to ensure latch-up does not occur [8].

D. FILTERS

A filter is normally situated between the voltage source and the rectifier. One can also be placed between the inverter and the load. The manufacturer determines that. Passive filters are made up of some combination of passive devices like inductors and capacitors. These devices are arranged such that the harmonic components are either attenuated through them or shunted into them. Three passive filter topologies are Series, Shunt, and Low-Pass Broadband Passive filters, illustrated in Figures 12–14 [12].

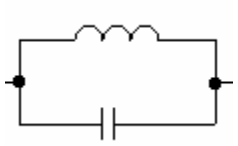

Figure 12. Series Passive Filter [From Ref. 12.].

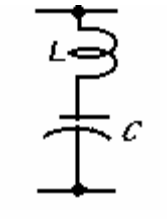

Figure 13. Shunt Passive Filter [From Ref. 12].

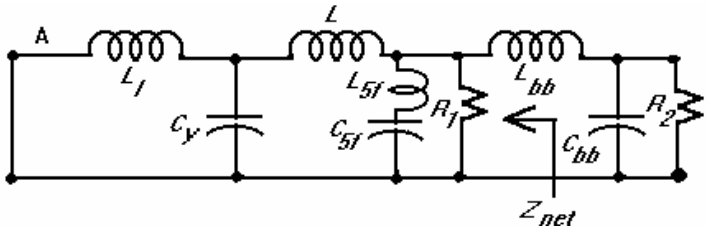

Figure 14. Simplified One-Line Representation of an Electrical Network with a Fifth Harmonic Tuned Filter and a Broadband Harmonic Filter [From Ref. 12].

There are drawbacks in the use of series and shunt passive filters. Series and shunt passive filters are effective only in a narrow proximity of the frequency at which they are tuned. A separate filter link is required for each harmonic frequency that needs to be filtered. Low–pass broadband passive filters have a broader bandwidth and attenuate almost all harmonics above their cutoff frequency.

A passive filter's impedance in relation to all other impedances gives the degree of filtering in the system. The degree of filtering will therefore vary according to variations in the network impedance. The amount of harmonic current absorbed by the filter is not controlled, but it is the result of the impedances, the generated harmonic current, and any harmonic distortion originating from the feeding system.

Passive filters can also generate reactive power. This means that the network characteristics need to be well known to allow the passive filter to be correctly sized. Consequences are that all later changes in the system will alter the behavior of the filter. Most AC drives have inherently high power factor, and so provide only small amounts of reactive power. Therefore attempting to filter the harmonics with reactive power generating passive filters tends to lead to overcompensation. [12]

There are also series and shunt active filters [12]. The series filter is typically a voltage–source inverter that acts as a controlled voltage source. The series active filter

does not compensate for load current harmonics. It presents zero impedance to the external circuit at the fundamental frequency but it acts as high impedance to the current harmonics coming from the power source side. The shunt active filter introduces a current waveform into the ac network. This current waveform, combined with the harmonic current, results in an almost perfect sinusoidal waveform. [12]

The majority of active filter topologies are complex and require active switches and control algorithms. Algorithms are implemented using Digital Signal Processing (DSP) technology. The active filter topology also needs current and voltage sensors and corresponding Analog-to-Digital (A/D) converters. This extra hardware increases the cost and component count, reducing the overall reliability and robustness of the overall ASD design [13].

The most promising filter topology is a hybrid combination of the passive shunt and active series filter. This design allows the active filter to be sized for only a fraction of the total load power, reducing costs and increasing overall system efficiency. The filter keeps the line current almost sinusoidal and in phase with the line voltage supply. It also responds very fast under sudden changes in the load conditions, reaching steady state in about two cycles of the fundamental [12].

E. CONTROL

A processor employing one of a variety of control methods manages the control of an ASD. There are two dominant control methods that are currently used in AC ASDs are scalar control and vector control. A less common control technique called adaptive control and is discussed in Chapter V.

The scalar control method has been the most popular because it is the least complex. The scalar control method, also known as constant volts per hertz, is an open-loop control system, which maintains a constant ratio between applied voltage and frequency. Scalar control is the least robust control method of the two. During steady–state operation, if the load torque is increased, the slip will increase within the stability limit and a balance will be maintained between the developed torque and the load torque. If the desired output frequency exceeds the base frequency of the motor, the voltage is held at

the rated value, ensuring less than rated flux flows through the core. Beyond motor base frequency, the motor transitions from the constant torque range to the field weakening range (also called the constant horsepower range), shown in Figure 15. In the constant horsepower range the peak motor torque capability is decreased [13].

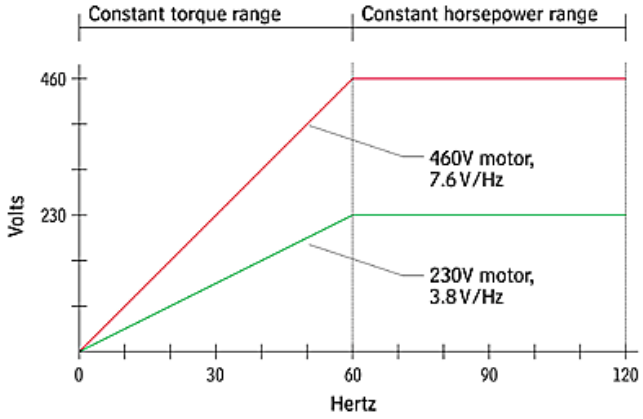

Figure 15. Volts/Hertz ratio [From Ref. 13.].

The vector control method is also known as field–oriented control. In vector control, the d-axis of the stationary reference frame for the motor is maintained on top of the rotating rotor flux. The resulting dynamic behavior is similar to that of a DC machine. This allows the AC motor's stator current to be divided into a flux–producing component and an orthogonal torque–producing component, similar to a DC machine field current and armature current. The key to vector control is knowledge of the rotor flux position angle with respect to the stator. It allows the motor to be controlled like a separately–excited DC motor. Vector control allows for fast transient response due to decoupling the torque and flux-producing currents. It also eliminates the conventional stability problem of crossing the breakdown torque point [14].

Vector control is further categorized into direct and indirect vector control. The basic difference between the two is that direct vector control requires a sensor to directly measure the flux. The flux is measured using flux sensing coils or Hall–effect devices. With indirect vector control the flux angle is estimated from the equivalent circuit model and from measurements of the rotor speed, the stator current and the voltage. One technique for estimating the rotor flux is based on the slip relation. This requires measure-

ment of the rotor position and the stator current. Given fairly accurate current and position sensors, this method performs reasonably well over the entire speed range.

The vector control method calls for fixed controller parameters. In a realistic drive system, plant parameters may vary which could lead to the deterioration of the system's performance. Adaptive control techniques have been developed to force the controller to adapt to the plant condition based on on-line extraction of plant information. Adaptive control calls for the use of a powerful microcomputer to implement the complex algorithms involved [14].

F. SIZE, WEIGHT, COMMERCIALLY AVAILABILITY

Size is a real concern as space is a valuable commodity aboard ship. Where the ASD will be installed must be taken under serious consideration. Table 1 shows the number of potential ASD applications aboard an Arleigh Burke destroyer. Obviously, large horsepower applications provide more opportunity for power savings. Table 2 and Table 3 list the size, weight, and cost for several ASDs available in the marketplace today. An analysis of two of these applications, the fire pump and chilled water pump, will be the focus of this thesis.

Application	Quantity	Motor Rating (HP)	VSD Rating (HP)
AC Chilled Water Plant Compressor	4	250	250
Fire Main Pump	6	150	150
Propulsion Gas Turbine Module Cooling Fan	4	130	150
Controllable Pitch Propeller Pump	2	125	150
Steering Gear Hydraulic Power Unit	4	100	100
AC Chilled Water Pump	4	60	60
Main Reduction Gear Lubrication Oil Service Pump	4	60	60
Centralized Seawater Cooling Pump	5	50	60
Anchor Windlas	1	50	60
Fixed Capstan	1	40	60
Ship Service Gas Turbine Module Cooling Fan	3	25	25
JP-5 Service Pump	1	20	25
CL W Vent Fan	1	20	25
CL Z Vent Fan	9	15	25
Ship Service Gas Turbine Generator Seawater Pump	3	10	10
Cold Potable Water Pump	2	10	10
Marine Diesel Oil Fuel Service Pump	4	7.5	10
VCHT Sewage Ejector Pump	4	7.5	10
CL Z Vent Fan	2	10	10
CL W Vent Fan	14	7.5	10
CL W Vent Fan	32	5	5
CL Z Vent Fan	9	3	3
CL W Vent Fan	8	2	3
CL Z Vent Fan	10	1.25	3
CL W Vent Fan	7	1	3
CL Z Vent Fan	3	0.75	3
CL W Vent Fan	6	0.5	3
CL W Vent Fan	9	0.25	3

Table 1. Potential ASD Motor Candidates [From Ref. 4.].

150 HP Applications					
	Alstom	Eaton	Rockwell Automation	Siemens	Conventional Motor Controller
Vendor Catalog #	MV3180A5A1	SV9150AGV-5M0A00	1336F-B125	6SE79032-1EG60Z+L20	Not Applicable
Size (in) (W)(H)(D)	(17)(34.4)(16.6)	(14.7)(39.4)(13)	(15)(48.8)(10.7)	(20)(57.1)(18.2)	(22)(30)(12)
Volume (ft^3)	5.6	4.4	4.6	12	4.6
Weight	221	221	240	341	197
Rough Delivered Cost	Nominal Cost - $20,000				$5,716
Additional Equipment Required	Insulator Input fuses Reactor	Input fuses	Input fuses	Input fuses	None
Packaging	Packaged to meet shock and vibration	Packaged to meet shock and vibration	Packaged to meet shock and vibration	Packaged to meet shock and vibration	No Additional
Cabling	none recommended	No special requirements	FOCUS Cable	none recommended	No special requirements
VSD Issues	Enclosure Temperature, Packaging to Meet Shock, Harmonics				None

Table 2. Potential ASD Cost, Weight, Size, and Manufacturers for 150-HP Applications [From Ref. 4.].

10 HP Applications					
	Alstom	Eaton	Rockwell Automation	Siemens	Conventional Motor Controller
Vendor Catalog #	MV3052A5A1	SV9010AGV-5M0B00	1336F-BRF75	6SE7021-8EB61	Not Applicable
Size (in) (W)(H)(D)	(6.7)(24.4)(13.8)	(4.7)(15.4)(8.5)	(10.3)(13.8)(8.4)	(5.3)(16.7)(13.8)	(14)(16)(8)
Volume (ft^3)	1.3	0.4	0.7	0.7	1
Weight	59.5	17.6	35	26.4	56
Rough Delivered Cost	Nominal Cost - $5,000				$1,750
Additional Equipment Required	Insulator Input fuses Reactor	Input fuses	Input fuses	Input fuses	None
Packaging	Packaged to meet shock and vibration	Packaged to meet shock and vibration	Packaged to meet shock and vibration	Packaged to meet shock and vibration	No Additional
Cabling	none recommended	No special requirements	FOCUS Cable	none recommended	No special requirements
VSD Issues	Enclosure Temperature, Packaging to Meet Shock, Harmonics				None

Table 3. Potential ASD Cost, Weight, Size, and Manufacturers for 10-HP Applications [From Ref. 4.].

Tables 2 and 3 show supplier recommended COTS ASDs currently available for the two different horsepower applications. The tables include catalog number, size, weight, rough cost, additional equipment required, recommended packaging, cabling, and identification of unresolved ASD issues. Additionally, data for the current existing motor controller is provided so that a comparison can be made. ASDs will continue to improve performance as technology improves. Issues such as power harmonics, Electro–Magnetic Interference (EMI), Radio Frequency Interference (RFI), shock, and vibration are a concern to many commercial applications as well as to the U.S.Navy. It is likely that future drives will incorporate EMI and RFI mitigation equipment that theoretically may put the drives below the military specification requirements in conjunction with shielded cables for connecting the drives to the motor control circuit. Currently, manufacturers package ASDs to meet specific installations' requirements. However, standard drives are likely to

be less susceptible to shock and vibration since many industrial applications require ruggedized packaging. As ASD performance increases, overall size, weight, and cost is expected to decrease.

G. CERTIFICATION OF COMMERCIAL UNIT

Any ASD system fielded by the U.S. Navy will have to comply with the following military standards. MIL-STD-1399 defines the power system operating criteria and the operating criteria of the user equipment connected to the power system. MIL-STD-1399 limits Total Harmonic Distortion (THD) to 3% for user equipment harmonic current and 3% for each individual harmonic. The system will also have to operate within MIL-STD-461 requirements for EMI mitigation. An ASD will typically require shielded cabling and specialized packaging to operate within MIL-STD-461 guidelines. Shock mounts will be needed in order to comply with MIL-S-901 shock and MIL-STD-167 vibration requirements. [4]

H. CHAPTER CONCLUSION

This chapter introduced the elements of an ASD and their theory of operation. The possible points of application for ASD technology aboard an Arleigh Burke destroyer were identified as well as the manufacturers who would be able to provide the ASDs. Standards that the ASDs must adhere to were also cited. Chapter III will discuss the technical challenges that have to be addressed before the consideration of investing in ASD technology.

THIS PAGE INTENTIONALLY LEFT BLANK

III. TECHNICAL CHALLENGES

A. INTRODUCTION

There are a number of obstacles that must be noted and overcome in order for the benefits of ASD to be achieved. Chapter III explains the technical challenges and gives possible solutions to overcome these challenges.

B. INPUT HARMONICS

Input harmonics are the result of the rectification of the source voltage supplied to the ASD. A harmonic is a component of a periodic signal with a frequency that is an integral multiple of the fundamental periodic signal frequency. THD is a measure of the contribution of all of the harmonic frequency components. THD is determined by

$$\%THD = 100 \times \sqrt{\sum_{h \neq 1} \left(\frac{I_{sh}}{I_{s1}} \right)^2}, \tag{3.1}$$

where I_{sh} is the component at the harmonic frequency, I_{s1} is the fundamental component and h is the harmonic. In order to determine the characteristic harmonics generated, the following formula is utilized: [15]

$$h = (n \cdot p) \pm 1, \tag{3.2}$$

where n is an integer, and p is the number of poles/rectifiers. For example, a six-pulse rectifier will produce odd, non–triplen, harmonics such as the fifth, seventh, eleventh, and thirteenth order harmonics. Nonlinear loads create harmonics by drawing current in abrupt short pulses, rather than in a smooth sinusoidal manner, demonstrated in Figure 16 below.

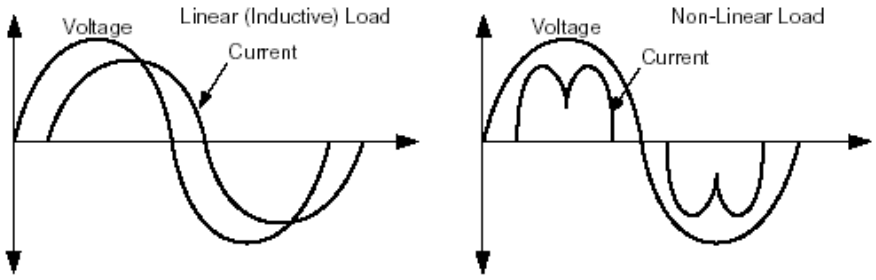

Figure 16. Differences between Linear and Non-Linear Loads [From Ref. 15.].

All ASDs create harmonics due to the switching of the inverter and the rectifier, which pulls power from the AC source. An example of distortion caused by the third harmonic is shown in Figure 17.

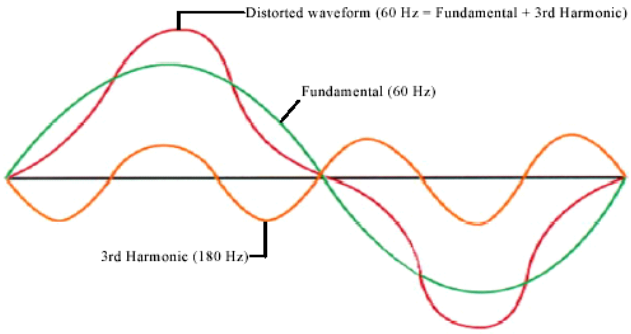

Figure 17. Waveform Composed of Fundamental and Third Harmonic: THD approximately 30% [From Ref. 16].

MIL-STD-1399 Section 300 Paragraph 5.2.8, entitled Input Current Harmonics, limits user equipment input harmonic current to 3% THD, and 3% for each individual harmonic [4]. The rationale for minimizing the current harmonics to this level was to protect the voltage waveform provided to all power system users. Harmonic currents on undersized conductors or cables can exhibit a "skin effect", which increases with frequency and can cause conductors to overheat [4]. If a capacitor is tuned to one of the characteristic harmonics such as the fifth or seventh, overvoltage and resonance can cause dielectric failure or rupture the capacitor. Harmonics can cause false or spurious operations and trips, damaging or blowing components for no apparent reason.

There are several methods for reducing harmonics. The most common is the addition of an isolation transformer. An isolation transformer allows one to "voltage

match" by stepping up or stepping down the system voltage, and by providing a neutral ground reference for ground faults. Another method is to increase the number of pulses or rectifiers, typically to twelve, thus eliminating the fifth and seventh harmonics and causing the eleventh and thirteenth harmonics to dominate. The disadvantages of these solutions are cost, construction, and weight. Examples of six-pulse and 12-pulse current waveforms are shown in Figure 18.

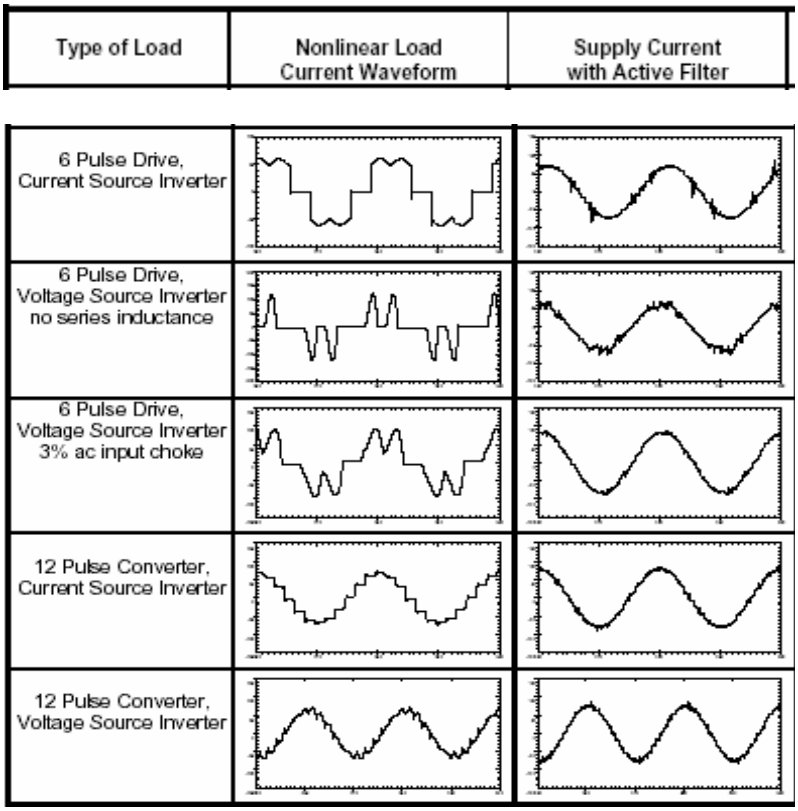

Figure 18. Six-pulse vs 12-pulse rectifier current waveforms [From Ref. 15.].

C. VOLTAGE TRANSIENT RESPONSE

The rapid rise of voltage associated with the chopping of a PWM inverter combined with impedance differences between the cables and the motor acts like a transmission line causing voltage reflection. This problem is of particular concern in a situation where there are long leads between the inverter and the motor. Cable length may not pose a significant problem in naval shipboard applications but still should be noted. Care should also be taken to match the impedance of the cable to the motor. As the pulses

reflect, they reinforce each other causing peak voltages on the cable and at the motor terminals that can be several times the nominal drive output voltage. As reflected waves encounter other waves, their values potentially add, causing higher peak voltage. This is shown in Figure 19.

High switching frequencies (2-20 kHz) are common with the present–day IGBT technology. Today's IGBTs switch at a speed of 100-200 ns. In a 460 V ASD system, IGBTs are fed by 650 V_{DC} and the rate of change of voltage with respect to time can exceed 7,500 V/ms [17].

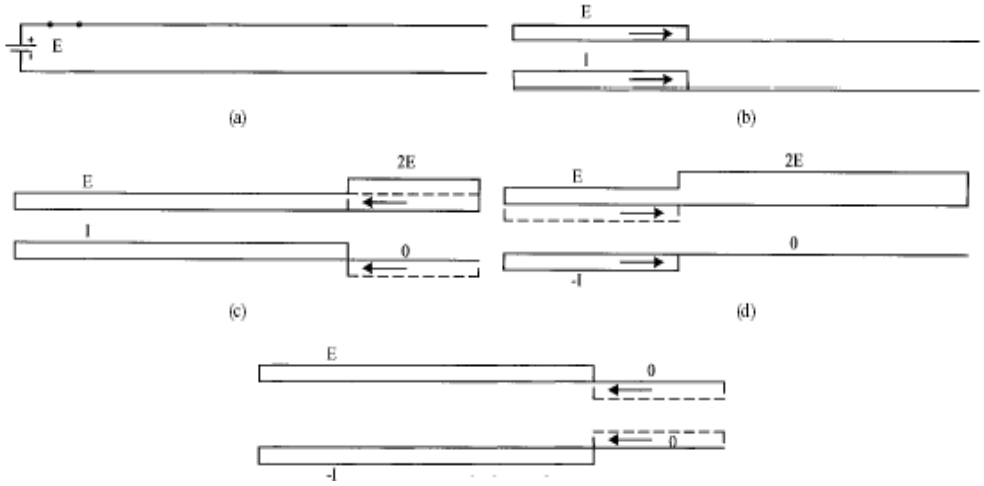

Figure 19. Repeated reflection steps [From Ref. 17.].

As the carrier frequency increases, more waves collide, increasing the number and level of voltage peaks. Since there is not sufficient dampening in wires, peak levels are reached. This causes rapid breakdown of motor insulation, leading to motor failure. Reflected voltage is a product of the voltage waveform and the voltage reflection coefficient, Γ [17].

$$\Gamma = \Gamma_L - \Gamma_S \tag{3.3}$$

The load and source reflection coefficients, Γ_L and Γ_S, respectively, can be expressed as

$$\Gamma_L = \frac{R_L - Z_O}{R_L + Z_O} \tag{3.4}$$

where R_L is the load resistance and Z_O is the characteristic impedance (or surge impedance) given by

$$Z_O = \sqrt{\frac{L_C}{C_C}} \tag{3.5}$$

where L_C is the cable inductance and C_C the cable capacitance. Then, the source voltage reflection coefficient is defined as

$$\Gamma_S = \frac{R_S - Z_O}{R_S + Z_O} \tag{3.6}$$

where R_S is the source resistance [17].

There are two primary means of reducing the motor insulation stresses due to motor terminal over-voltages: 1) filtering techniques or 2) increasing the insulation strength of the magnet wire to withstand a large voltage transients (i.e., high *dv/dt*). A specially–designed shunt filter installed at the motor terminals has been shown to effectively dampen the voltage over–shoot. The primary role of the inverter output filter is to reduce the *dV/dT* of the inverter output pulses below a determined critical value, such that overvoltages do not occur at the motor terminals. The filter size, cost, weight, and losses are optimized. Figure 20 shows that increasing the rise time of the PWM inverter output voltage that is applied to the cable at a critical value will significantly reduce overvoltages due to reflections. For example, a PWM inverter output voltage rise time of 3.9 microseconds on a 50-ft cable corresponds to a normalized peak motor voltage of 1.1 and a rise time of 0.5 microseconds in the same cable corresponds to a normalized peak motor voltage of 1.5.

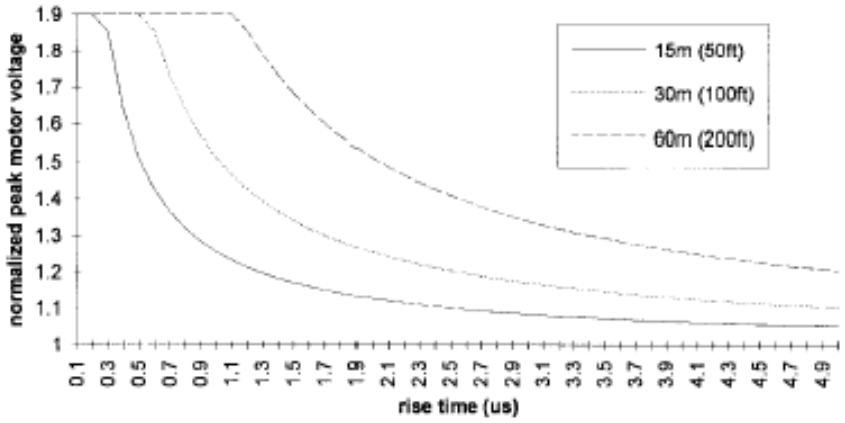

Figure 20. Normalized Peak Motor Voltage vs. Rise Time [From Ref. 17.].

Thus, a low–pass filter, as shown in Figure 21 below, placed at the output terminals of the inverter can be specially designed to slow down the inverter output pulse rise time, and therefore, significantly reduce the overvoltage and ringing at the motor terminals.

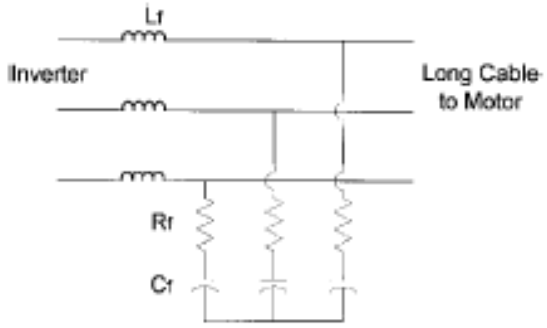

Figure 21. Inverter Output Low-Pass Filter [From Ref. 17.].

There are several low–pass polynomial filter configurations with different shapes of amplitude-versus-frequency responses. The topology in Figure 21 would reduce the V^2/R power losses across the damping resistor. The second–order filter is found to yield the necessary stopband attenuation characteristics and the maximum ripple values in the passband.

The transfer function, *H,* that defines the behavior of the network is

$$H = \frac{V_o}{V_i} = \frac{1 + j\omega R_f C_f}{1 - \omega^2 L_f C_f + j\omega R_f C_f} \tag{3.7}$$

where V_o is output voltage, V_i is the input voltage, R_f is the filter resistance, C_f is the filter capacitance, and L_f is the filter inductance The effective attenuation, A, in decibels is

$$A = 20\log\left|\frac{1}{H}\right|. \tag{3.8}$$

Figure 22 and Figure 23 show the line–line voltage of an inverter without and with the filter [17].

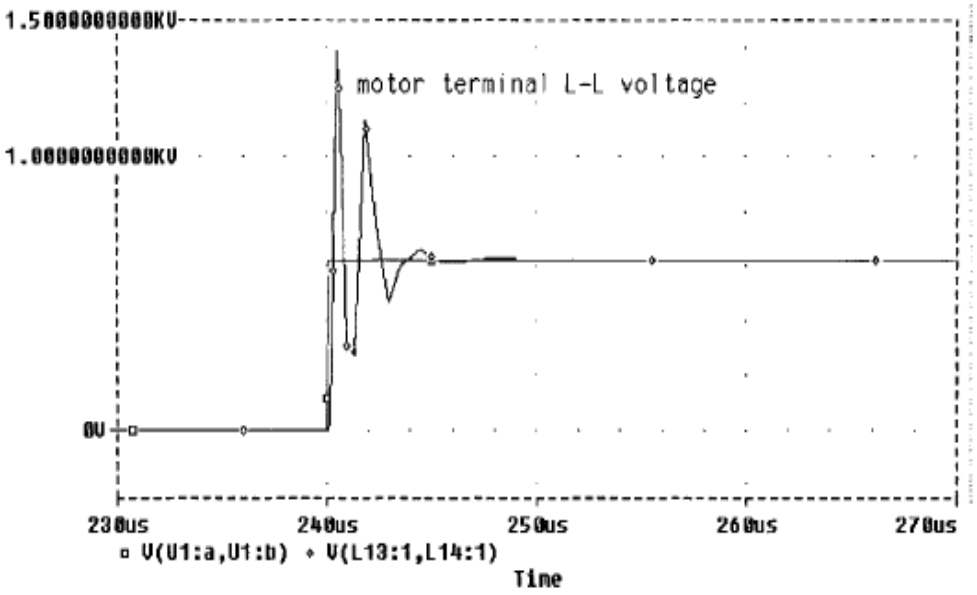

Figure 22. Inverter Output Pulse and Motor Terminal L–L Voltage without Filter for 460V, 5-kVA, 2-kHz ASD with 100-ft Cable. [From Ref. 17.].

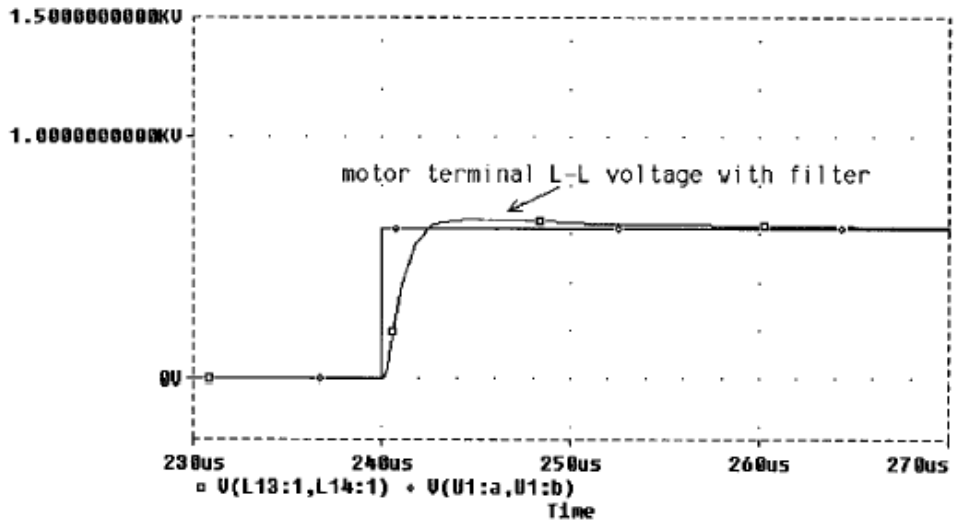

Figure 23. Inverter Output Pulse and Motor Terminal L–L Voltage with Filter for 460V, 5-kVA, 2-kHz ASD with 100-ft Cable. [From Ref. 17.].

It is clear that the filter has a profound effect upon the output voltage.

D. ELECTROMAGNETIC INTERFERENCE (EMI)

EMI is an undesirable effect caused by the application of ASDs. EMI signals are transmitted via conduction or radiation. EMI affects other electronic instruments, causing them to fail or operate outside of their design parameters. EMI is considered to consist of two parts, the common-mode and differential-mode components. The inductance of the motor windings provides a very large impedance in the frequency range of the conducted EMI, which is in the 150 kHz–30 MHz range. There is also unintended stray capacitance between the motor windings in the range 2–10 nF. These come together to provide an alternative low impedance path for both common-mode and differential–mode noise currents. The common-mode noise current flows through the stray capacitance inside the motor to the ground and back to the input terminals of the converter through the power mains. The differential-mode noise currents flow between the motor phase windings and through the stray capacitance inside the motor back to the power mains via the DC bus and the rectifier, causing the differential-mode conducted EMI [18]. An Arleigh Burke destroyer has a delta-wired electrical system, meaning that the electrical equipment aboard do not share a common earth ground. In order to prevent common-

mode noise from entering the ship's electrical grid, shielded power cables should be employed. Figure 24 shows an EMI induced current path.

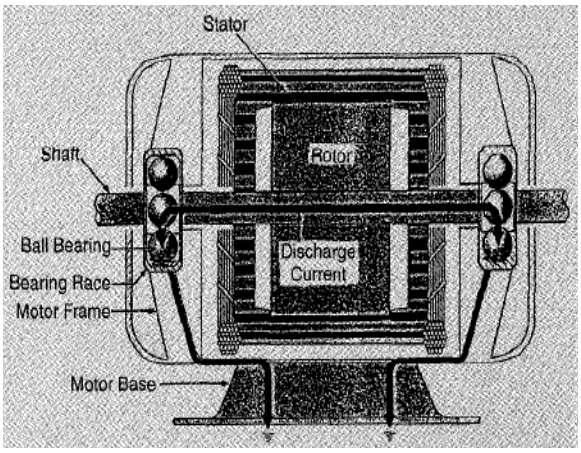

Figure 24. Electromagnetic Induced Circulating Current [From Ref. 19.].

The most effective means of preventing EMI emissions is a snubber circuit. A snubber prevents EMI at the source. The more common approach is the use of filters. A filter consisting of high frequency inductors and capacitors are used to reduce the high-frequency noise. The inductors act as open circuits and the capacitors act as short circuits at high frequencies [8]. A 60-dB reduction in noise is usually what is desired.

E. BEARING CURRENTS

The useful lifetime of a bearing in industrial applications is typically 20,000–40,000 hours. These bearings in general remain mechanically viable out to 40,000–60,000 hours. Bearing failures may be caused by mechanical vibration, thermal overload, or the conduction of electrical currents. Recent studies suggest possible mechanisms for bearing damage when operating on ASDs are *dv/dt* induced currents and oil film dielectric breakdown with Electrical Discharge Machining (EDM) currents. Modern PWM inverters switch a DC bus voltage, V_{dc}, onto the three–phase terminals of the motor in a switching pattern that creates the proper fundamental component voltage and frequency. The average voltage applied to the motor is kept to zero, unlike the instantaneous sum of the voltages at the motor terminals, which is nonzero. This instantaneous voltage sum is called the common–mode voltage. Common–mode voltage is found between the motor windings and motor ground. Most rectifiers that create the V_{dc} also introduce a com-

mon–mode voltage onto the V_{dc}. This voltage exists between the motor windings and the motor ground. It contains high rates of change of voltage with respect to time (i.e., high *dv/dt*). The high *dv/dt* creates frequency content in the common–mode voltage in the MHz range. This is a problem for areas where capacitance would normally act as a type of insulator in regular electric motors [19].

All rotating machines, DC or AC, develop bearing currents, large or small horsepower. It has been understood for quite some time that rotor voltages caused by asymmetries inherent in the motor construction produce bearing currents. The rotor voltage induced along the axial length of the machine produces a circulating current whose magnitude is mitigated by the bearing impedance. The electro–magnetic induced circulating current path in Figure 24 is from one end of the shaft, through the impedance of the bearing to frame ground, back through the opposite bearing impedance, and returning back to the shaft [19].

Bearing impedance is low at low speeds and attains values in the Mega-ohms range as motor speed increases above 100 rpms. NEMA regulations require the maximum shaft voltage must be less than 1 V_{rms} with 60-Hz AC line operation. A shaft voltage of 1 V_{rms} is considered safe and not likely to cause bearing currents that would lead to fluting. Initially, bearing damage begins with the formation of small pits or fusion craters in the bearing races as shown in Figure 25 [19].

Figure 25. Fusion Craters in a Bearing Race from Scanning Electron Microscope Image. [From Ref. 20.].

As this continues, a fluting pattern develops that may or may not incorporate fairly regular spacing. Figure 26 shows a pattern of fluting on a bearing race.

Figure 26. Bearing Race Fluting. [From Ref. 20.].

The resulting lubrication breakdown and mechanical wear ultimately lead to bearing failure. The ball bearings of these motors ride on a lubricating oil film (typically 0.2–2 μm depending on the rpms). This film acts as a capacitor that gets charged by the rotor voltage. When the voltage applied to the oil film capacitor exceeds the voltage capacity of the film or when contact is achieved between ball bearing asperity point and the raceway in a small area, a destructive instantaneous high discharge current, previously referred to as EDM current, takes place. The result is usually a pitting of the ball bearings. This is more of a concern for AC motors with a high horsepower rating. In the past this phenomenon was countered by placing insulated ball bearings on the non–drive end, thereby inserting more capacitance in series with the bearing. ASDs with their PWM inverters excite an electrostatic capacitive effect between the stator and rotor, creating rotor shaft voltage to ground, V_{rg}. The stator neutral-to-ground voltage, V_{sng}, for a 60 Hz, 460 V_{rms} source on a sine wave operation of a standard motor is in the range of 30 V peak [19]. On the other hand V_{sng} on ASDs can possibly reach hundreds of volts due to PWM modulation, as evidenced in Figure 27.

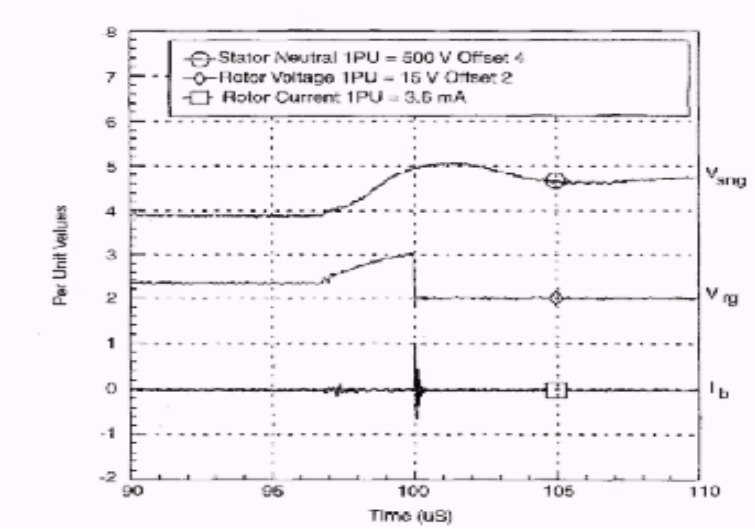

Figure 27. Graph of V_{sng}, V_{rg}, and I_r [From Ref. 19.].

Maximum V_{sng} is a zero sequence source of approximately $V_{bus}/2$, but may allow transient edges of higher values associated with common-mode components and long cable runs. Now the common–mode voltage of the ASD's modulator, the coupling impedance between the stator and rotor and the bearing impedance determines V_{rg}. These factors may now allow the ASD to produce sufficient V_{rg} to cause EDM currents that in turn increase bearing wear. There are several design proposals that seek to eliminate or at least reduce shaft voltage. One of the more promising designs is the Electrostatic Shielded Induction Motor (ESIM) depicted in Figure 28.

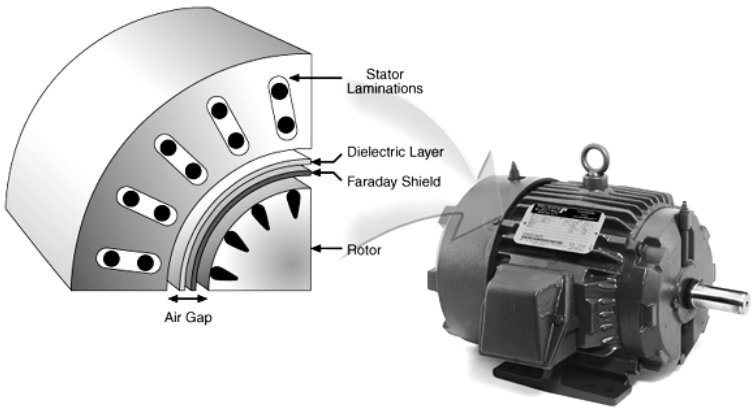

Figure 28. Electrostatically Shielded Induction Motor [After Ref. 20.].

The ESIM has a Faraday shield. The Faraday shield blocks the electrostatic coupling between the stator and the rotor and thus prevents the shaft voltage from building

up by shunting it to ground. The motor's electro–magnetic torque is unaffected by the shield. It does not impede the magnetic field coupling. Some results of the ESIM design can be seen in Tables 4–6.

Table 1. Rotor Shaft Voltage Attentuation Comparison with Open Circuited Bearings

	ESIM with Copper Tape			ESIM with Copper Slot Stick Covers at No Load			ESIM with Copper Slot Stick Covers at 100% Load		
Test Machine	Rotor Voltage (V peak)	Attenuation Reduction	Expected Attenuation	Rotor Voltage (V peak)	Attenuation Reduction	Expected Attenuation	Rotor Voltage (V peak)	Attenuation Reduction	Expected Attenuation
Standard Machine	40	0%	0%	19	0%	0%	16	0%	0%
ESIM with stator shield	18	56%	62%	12	37%	57%	8.5	47%	57%
ESIM with full shield	2.2	95%	100%	1.7	91%	100%	1.5	91%	100%

Table 4. Rotor Shaft Voltage Attenuation Comparison with Open Circulated Bearings [From Ref. 19.].

Table 2. Effectiveness of ESIM: Voltage and Current Comparison

Test Motor	Rotor Voltage	dv/dt Current	EDM Current
Standard Machine	10 V peak	500 mA peak	3.5 A peak
ESIM with copper tape on the stator length	10 V peak	18 mA peak	none
ESIM with copper tape on stator and end winding	2.2 V peak	17 mA peak	none

Table 5. Effectiveness of ESIM: Voltage and Current Comparison [From Ref. 19.].

Table 3. Calculated Bearing Life with PWM IGBT Drives and 15 hp Motor					
		Standard Motor		ESIM Motor	
Parameter	Units	Rotor Weight	3 Times Rotor Weight	Rotor Weight	3 Times Rotor Weight
EDM Current	A peak	2.2	2.2	0	0
– Contact Area	mm^2	0.62	1.29	0.62	1.29
– Current Density	A peak/mm^2	3.5	1.7	0	0
– Calculated Life	hours	< 10	1,570	> 100,000	> 100,000
dv/dt Current	A peak	0.2-0.5	0.2-0.5	0.05	0.05
– Contact Area	mm^2	0.62	1.29	0.62	1.29
– Current Density	A peak/mm^2	0.32-0.8	0.15-0.38	0.08	0.04
– Calculated Life	hours	> 100,000	> 100,000	> 100,000	> 100,000

Table 6. Calculated Bearing Life With PWM IGBT and 15-HP Motor [From Ref. 19.].

The tables show that the ESIM introduces a significant improvement in the performance of the induction motor. The outcomes approached NEMA guidelines for conditions allowing for reasonable bearing life.

F. COOLING

The premise in using ASDs is that the motor will operate at a variety of speeds in order to do the required task. This variation in speed will significantly affect the heat transfer efficiency. Cooling fans whose rotation is directly supplied by the motor are subject to high windage losses and noise at high speeds. ASDs are designed to operate across a very wide frequency range. This may place the motor cooling fan well above its fixed-frequency-design operating point and that often leads to inefficient airflow and unacceptable noise levels. In constant–torque applications, the motor's temperature limits will more than likely be exceeded. An option is to have an independently powered blower provide an essentially constant heat transfer rate.

The operating temperature of the motor is established by how efficiently the heat generated in the motor can be conducted to surfaces that are in contact with the cooling medium and the ability to transfer this heat through convection. A widely accepted estimate is that for every 10°C cooler a motor operates, its insulation life is doubled [20].

Square laminated-framed AC motors are being used to improve heat transfer. The laminated-frame design eliminates the stator-to-frame interface. Integral cooling ducts trap the air in contact with the frame along the motor's length. It provides a more direct and effective heat transfer path to the cooling air. [20]

G. CHAPTER CONCLUSION

The technical challenges of implementing ASD technology were identified and the reasons they are problematic for electrical systems seeking to take advantage of ASD technology explained. Chapter III also proposed solutions to overcome the obstacles such as isolation transformers and ESIM motors. Chapter IV categorizes the type of pumps used aboard the destroyer and describes the conventional methods of throttle control of pump systems.

THIS PAGE INTENTIONALLY LEFT BLANK

IV. PUMP SYSTEMS

A. INTRODUCTION

A pump is a device used to compress, drive, raise, or reduce the pressure of a fluid by way of a piston or set of rotating impellers. Pumps fall into two general categories, positive displacement pumps and dynamic (centrifugal) pumps. In this chapter positive displacement and centrifugal pump operation is explained. The methods for throttling flow through a system are discussed.

B. PUMPS

Positive displacement pumps seal water in a chamber, and then force it out by reducing the volume of the chamber. Most positive displacement pumps employ a reciprocating motion to impart waves of pressure causing dramatic changes in fluid velocities between strokes. Positive displacement pumps have a constant-torque characteristic [22].

Centrifugal pumps are variable torque devices. A centrifugal pump's impeller is coupled to the motor shaft. The impeller provides the kinetic energy to the fluid. The faster the impeller revolves or the bigger the impeller, then the higher the velocity of the liquid and the greater the energy imparted to the liquid. The momentum produced causes an increase in pressure or flow at the pump outlet. The candidate pumps aboard the Arleigh Burke destroyer are centrifugal pumps [22].

C. MECHANICAL CONTROL OF SYSTEM FLOW

A valve or any other mechanical means of controlling the flow has no direct control of pump output, as can be seen in Figure 29. With the pump operating at a fixed speed, at any given flow rate the pressure required by the process is lower than the pressure developed by the pump.

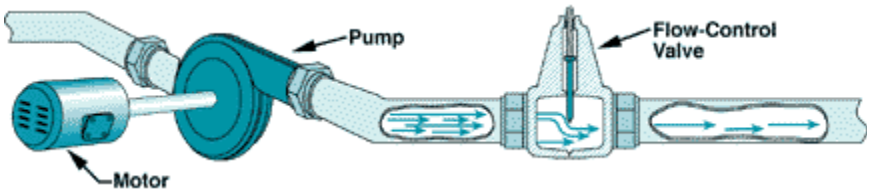

Figure 29. Model of Conventional Process Control [From Ref. 23].

The only exception is at the Natural Operating Point (NOP). The NOP occurs at the intersection of the system curve and the pump curve [24]. Figure 30 shows the NOP for the firemain system. The system, pump, and pump bhp curves were obtained from Ref. 4.

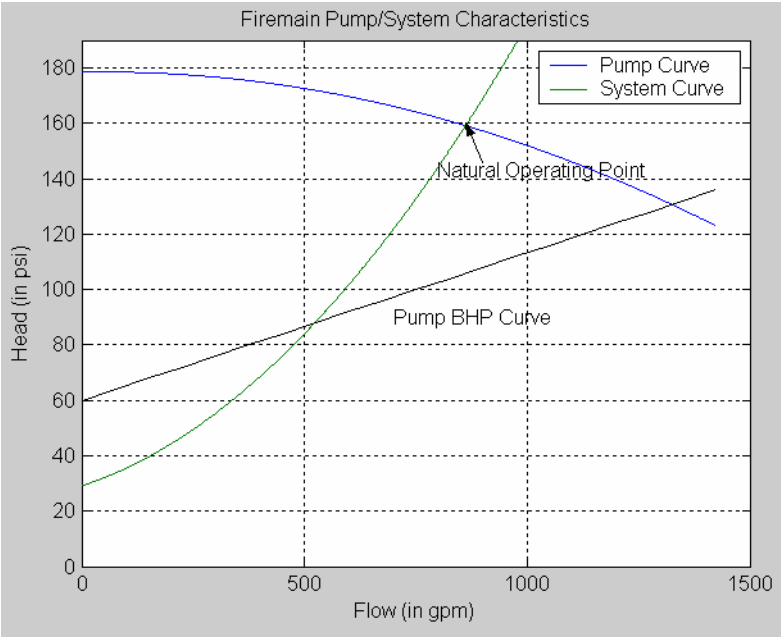

Figure 30. Firemain Pump System Characteristic [After Ref. 4].

To match the pressure requirement of the process, control valves are employed to either directly drop the excess pump pressure or indirectly drop the pump discharge pressure. Directly dropping excess pump pressure is known as output pressure throttling. This is achieved by inserting the valves between the pump discharge and the process, shown in Figure 31. A device that drops pressure and has flow through it consumes power. This power must be supplied by the electric motor driving the pump [24].

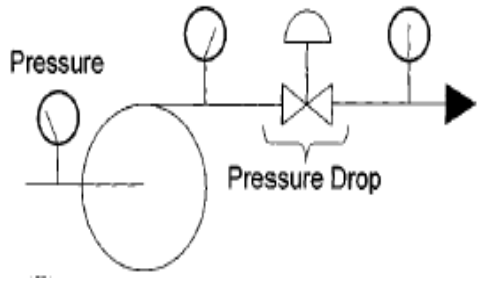

Figure 31. Output Pressure Throttling [From Ref. 23.].

Indirectly dropping the pump discharge pressure, the control valve recycles additional flow through the pump, as shown in Figure 32. This technique takes advantage of the fact that there is an inverse relationship between pump discharge pressure and flow. The control valve increases the flow through the pump body to a point where the pump discharge pressure matches that of the system requirement. The brake horsepower, bhp, requirement of the pump has a proportional relationship to flow, so the electric motor must supply this additional horsepower. Both output pressure throttling and recycling are extremely inefficient, but, of the two, recycling is the worst.

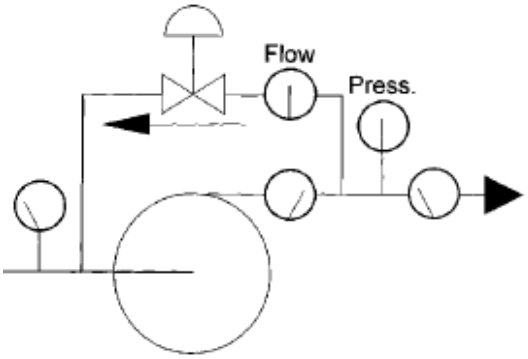

Figure 32. Recycling [From Ref. 23.].

A pump's output is solely determined (while running at full speed) by where it is operating on the pump performance curve. This means that line–side pressure increases in low-flow conditions as evidenced in Figure 30. When a high–flow condition occurs it should be noted that the device presents severe head loss translating into pressure loss on the load side of the valve. Therefore the pump must be sized to account for the extra head loss at high-flow conditions. Higher pressure for the designed flow rate equals more horsepower and that makes mechanical control inefficient. (This argument does not

hold if the pump or fan is allowed to operate at close to the maximum flow rate constantly, but this is rarely the case in shipboard applications.) Components of control valve architecture such as filters, orifices, and pilots containing mechanical springs are high maintenance items.

D. GAINS FROM ASD CONTROL

Generally a pump chosen for any application is more powerful than normally needed to accomplish its task. This is done in anticipation of a worst-case load scenario to try to ensure that the operation of the system is not interrupted. ASDs allow pumps to be operated at reduced load/speed based on the ship's current operational requirements. The ability to operate at speeds necessary to do the job at hand reduces structureborne, fluidborne, and airborne noise and reduces the overall noise signature of the ship. As the threats of the future are anticipated to be located more and more inside littoral waterways, this reduction in radiated noise will greatly enhance the ability of the navy to prosecute these threats while minimizing the threat to its own vessels. As an example there are total of 34 high capacity/velocity pumps aboard Arleigh Burke destroyers, Flight II class. Each pump would benefit acoustically if fitted with an ASD system. Table 7 list of those pumps:

Unit	Motor Rating	Quantity
Fire Pump	150 hp	6
Centralized Sea Water Cooling Pump	150 hp	5
Chilled Water Pump	250 hp	4
Hydraulic Oil Power Module Pump/Motor	100 hp	2
SSGTG Sea Water Cooling Pump	10 hp	3
VCHT Pump	7.5 hp	8
Lube oil Service Pump	60 hp	4
Potable water Service pump	10 hp	2

Table 7. Potential Candidate Pump Applications for ASDs [After Ref. 4.].

There are 63 vaneaxial fans and 32 Fan Coil Assemblies on DDG 79. Ventilation fans are one of the principle sources of airborne radiated noises aboard ship. Noise emanates from the air ducts as breakout noise or from the diffuser where the air discharges into the space. It has been determined that a 10 percent reduction in air flow will still allow the system to meet the cooling requirements for a shipboard compartment while reducing the noise level by 2–3 dB. This is significant as there are a number of spaces aboard the Arleigh Burkes where the noise radiated by the HVAC system exceeds acceptable levels by only few dBs. A good example of how an ASD fitted fan can improve the noise level within a space is the crew's mess. Currently the HVAC noise exceeds Arleigh Burke's Ship Specification Category B noise limits. Figure 33 demonstrates the predicted reduction in noise in the crew's mess if an ASD fan was used.

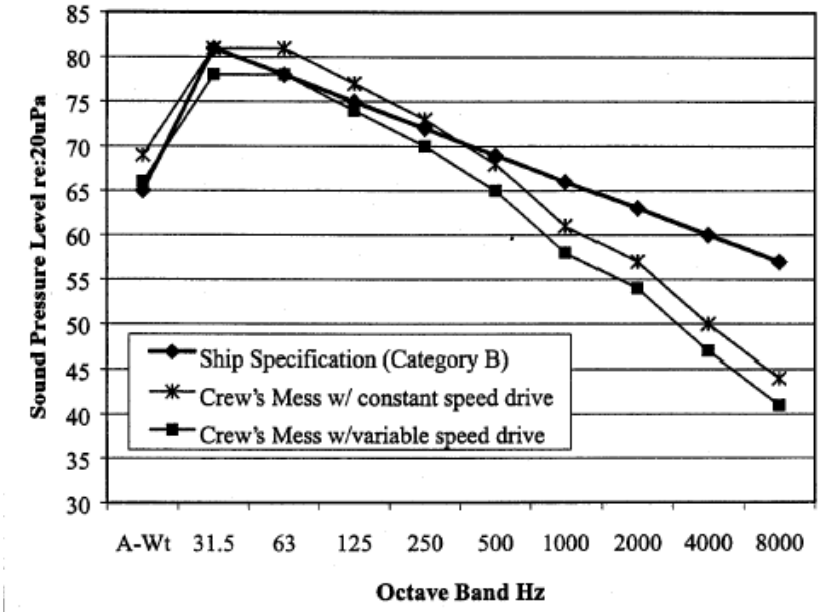

Figure 33. Crew's Mess Predicted noise Levels W/ASDs [From Ref. 4.].

E. CHAPTER CONCLUSION

Chapter IV introduced positive displacement and centrifugal pumps. The methods of control for conventional throttle pump systems were explained and the reasons for seeking an alternative method of control explored. Chapter V will demonstrate the potential power savings and operational cost savings associated with the implementation of ASDs.

THIS PAGE INTENTIONALLY LEFT BLANK

V. APPLICATIONS OF ASD TO CANDIDATE SYSTEMS

A. INTRODUCTION

There are numerous potential candidate systems for shipboard ASD implementation. The firemain and chilled water systems were chosen for this study. Descriptions of the systems along with their operating parameters are cited. MATLAB was used to demonstrate power savings and fuel cost savings.

B. CANDIDATE SYSTEMS

1. Firemain

The firemain system provides seawater to all hose connections and sprinkl–ing/deluge systems. It also provides seawater to the countermeasure washdown system, the desalinators, Close In Weapon System (CIWS) cooling, and drainage eductors. The firemain is configured as a vertical loop with an upper main on the starboard side along the damage control deck and a lower main on the port side along the second deck. Each main is supplied by three 1,000 gpm, Navy-Standard Titanium Fire Pumps (NSTFP). The fire pumps are required to maintain a minimum system pressure of 150 psi. [25]

The firemain system is composed of seamless pipe that is class 200, 90-10 copper nickel alloy in accordance with MIL-T-16240. Eight-inch diameter piping is used for the mains and cross connections, while six-inch diameter piping is used for the fire pump risers and the 02 level cross-connect. The firemain system worst-case scenario capacity is 6,000 gpm. The normal continuous service load demands on the system are far below this capacity. [25]

Cruise	Flow (gpm)
CIWS No. 1	25
CIWS No. 2	25
Steering Gear Coolers 1A & 2B	24
Starting Air Cooler	90
Fuel Oil Compensating System	110
Total	274
PCV Flow	230
Total Pump Flow	504

Table 8. Firemain flow requirement in underway cruise condition [From Ref. 4.].

2. Chilled Water

The tons of electrical equipment aboard an Arleigh Burke destroyer generate a lot of heat. The chilled water system aboard the ship removes that heat by acting as a primary coolant for the electronic equipment acting in concert with the HVAC system. The chilled water system provides cooling to fan coil assemblies, fan coil units, cooling coils, gravity coils, and unit coolers throughout the ship. The system is designed to supply water at a temperature of 44˚ Fahrenheit [26]. The coils regulate the air temperature and dehumidify the ship's internal environment. The vital systems aboard ship have both primary and alternate chilled water sources from both chilled water loops. They also are cooled by multiple coils or have primary and alternate sources of chilled water. Table 9 list some Combat Systems equipment that is cooled by the chilled water system.

System	**Gallons/Minute**	**Tons**
C&D Cooler	140	39.25
Sonar Cooler	36	14.62
AN/SPY 1-D Arrays	100	30.28
AN/SLQ-32	20	12.09
TACTAS	10	2.59

Table 9. Combat Systems Equipment Served by Chilled Water System [After Ref. 26.].

The system consists of four 200-ton air conditioning plants, four pumps, and three 750-gallon tanks. The pumps are rated for 900 gpm at 70 psi with a static head pressure of 5 psi. There are port and starboard supply and return headers for the coolant. These headers are cross connected forward and aft. The main isolation valves segregate the

system into two separated zones and provide damage control closures. Figure 34 shows a diagram of the chilled water system [26].

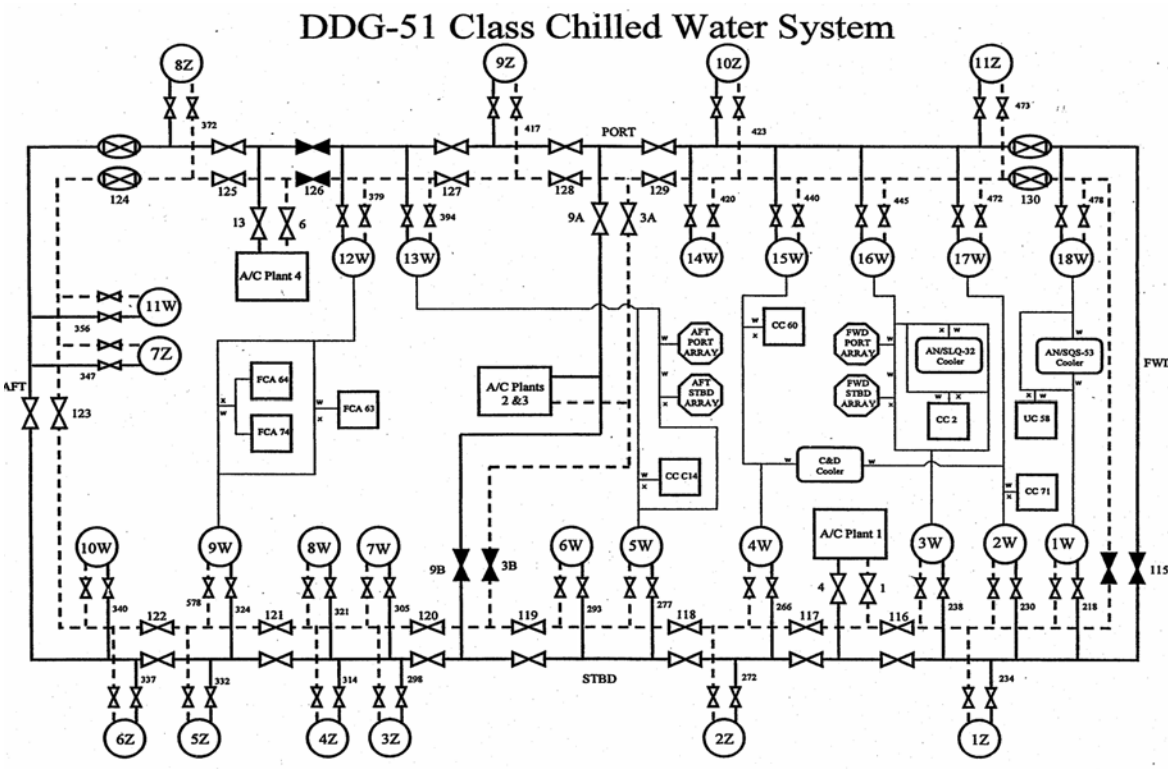

Figure 34. Arleigh Burke destroyer chilled water system [From Ref. 26.]

C. CALCULATING THE COST ADVANTAGES AND DISADVANTAGES OF ASDS

In order to ensure that ASD installations are right for the navy, an accurate accounting of the potential savings is essential to make certain the additional capital cost of ASD installations will yield an adequate return on the investment. The pump formulas that are used to determine the savings are simple, but they are easily misapplied. These errors tend to overestimate the energy savings. The systems must be mathematically modeled so that the pump hydraulic formulas can be properly applied [23]. Figure 30 shows that typically the pump characteristic is not compatible with the system requirements. The process system requires less pressure for reduced flow while the pump discharge pressure increases at reduced flow. As the flow requirement is reduced, there is an ever-increasing overpressure that must be dealt with. Fixed-speed pump methods tend to waste electrical power in dealing with this overpressure. If a NOP could be attained at

any flow rate, the wasted power associated with the over-pressures would be eliminated. This can be accomplished by changing the speed of the pump impeller with an ASD. The "fan laws" or "affinity laws" govern the relationship between the speed of the impeller, head (or pressure) developed by the pump, and the input power to the pump commonly referred to as brake horsepower, bhp [24].

$$\frac{Q_1}{Q_2} = \frac{N_1}{N_2} \tag{5.1}$$

and,

$$\frac{H_1}{H_2} = \left[\frac{N_1}{N_2}\right]^2 \tag{5.2}$$

and,

$$\frac{BHP_1}{BHP_2} = \left[\frac{N_1}{N_2}\right]^3 \tag{5.3}$$

where Q is the pump discharge flow rate (in gal/min), N is the pump impeller speed (in rpm), H is the pump discharge head (in ft or psi), BHP is the pump shaft input horsepower (in bhp), subscript "1" designates the initial conditions, and subscript "2" identifies the final conditions.

In order to properly assess the level of electricity savings associated with using speed control, the brake horsepower in both the fixed-speed and the adjustable-speed case must be determined for the various flows under consideration. For fixed-speed systems the pump manufacturer's flow versus horsepower curve, like in Figure 30, is used or the power into the motor is measured and factored in with motor efficiency. Adjustable-speed systems are more complex. The errors that are made typically overestimate the power savings. It is very important to understand that the variables within the affinity formulas are not independent of one another. A change in the pump's speed, changes all of the affinity formula variables. The result is that the horsepower prediction is usually too low.

To find BHP_2, an affinity curve is developed. The first step is locating where the final flow condition intersects the system curve. Then its corresponding final head pres-

sure can be identified. By using these results the affinity curve can be plotted. The manipulation of (5.1) and (5.2) yields [24]

$$\frac{H_1}{H_2} = \left[\frac{Q_1}{Q_2}\right]^2 \tag{5.4}$$

which leads to

$$H_1 = H_2 * \left[\frac{Q_1}{Q_2}\right]^2 . \tag{5.5}$$

Using (5.5) and the data from Figure 30 the affinity curve is obtained and is plotted in Figure 35.

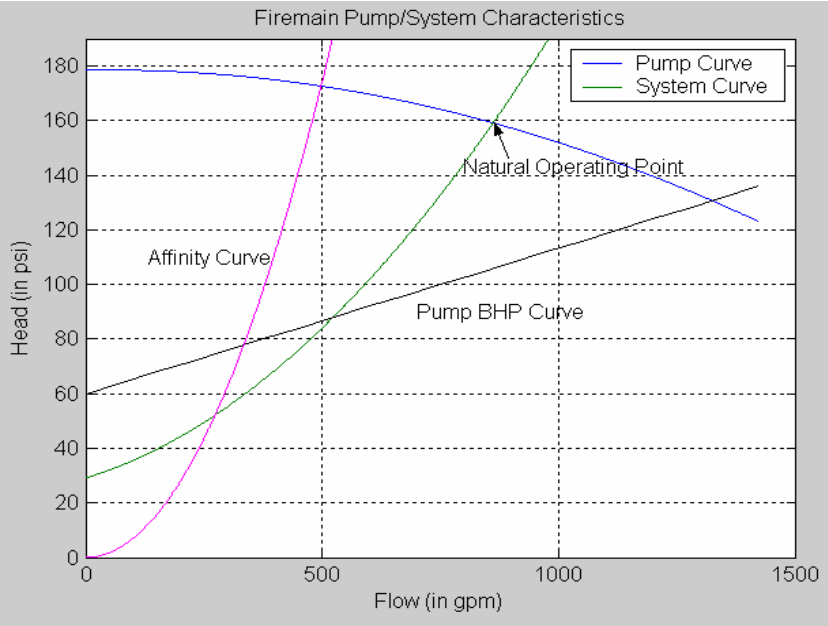

Figure 35. Firemain Pump/System Characteristic with Affinity Curve [After Ref.4.].

In Figure 35:

- The Pump, System, and Pump BHP Curves are from Ref. 4;
- The Natural Operating Point for the firemain is identified at the intersection of the system and the pump curve;
- The desired flow, Q_2, is determined by the application's requirement. The horizontal axis is entered at that value;
- The needed head pressure is identified by moving up vertically to the system curve and reading the Head value, H_2, of this intersection;

- Knowing Q_2 and H_2 Eq. (5.5) is then used to calculate and plot H_1 vs. Q_1 (the affinity curve).

Where the affinity curve intersects the pump curve will be the initial flow and head conditions. We then move vertically down to the Pump BHP curve. That intersection gives BHP_1. With BHP_1, Q_1, and Q_2, Eq. (5.1) can be substituted into Eq. (5.3) to calculate BHP_2 as

$$BHP_2 = BHP_1\left(\frac{Q_2}{Q_1}\right)^3. \tag{5.6}$$

Figure 36 considers an example; currently the firemain pump aboard an Arleigh Burke destroyer under normal cruise conditions provides 504 gpm of flow through the system. A flow of 274 gpm is needed to provide cooling for various ship systems. (The remaining 230 gpm is wasted through the utilization of the pressure control valve.) The following results are obtained when the savings gained by implementing ASD technology into the firemain system is calculated. A final flow, Q_2, of 274 gpm was desired. From the system curve at that value of flow a minimum final head pressure, H_2, of 52 psi would be needed. Knowing Q_1 and H_2, Eq. (5.5) can be used to calculate and plot the affinity curve. The new initial conditions at the intersection of the affinity curve and the pump curve are H_1 equal to 172 psi and Q_1 equal to 500 gpm. Moving vertically down from that point to the Pump BHP curve gives an initial brake horsepower, BHP_1, of 87 bhp.

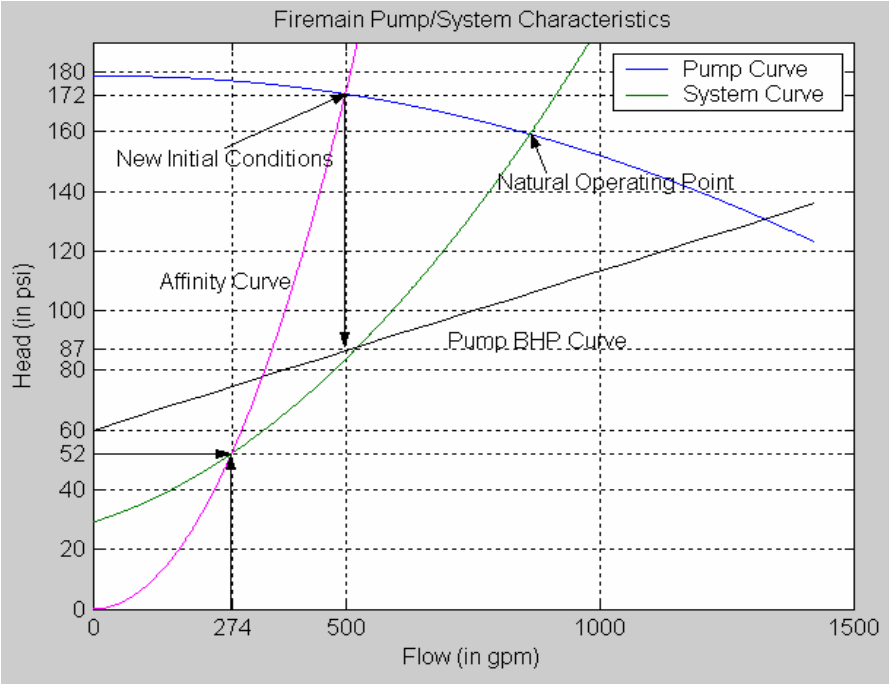

Figure 36. Graph of New Initial Conditions [After Ref. 4.].

The final brake horsepower was determined using Eq. (5.6) and it yielded a BHP_2 equal to 14.32 bhp. The system will have a flow of 274 gpm at 14.32 bhp but with a system pressure of only 52 psi. But the firemain pump must maintain a system pressure of 150 psi. So more input power is needed in order achieve the required pressure. The pump and BHP curves were scaled by $\left(Q_2^2/Q_1^2\right)$ to account for the reduction in motor speed, producing the scaled curves in Figure 37. The scaled pump curve is based on a pump discharge pressure of 160 psi. 160 psi was chosen to ensure that the required system pressure of 150 psi is maintained. Moving down vertically from a pump head pressure of 160 psi to the Scaled BHP curve the required brake horsepower, BHP_2, is 65 bhp. So the overall savings is

$$BHP_{saved} = BHP_1 - BHP_2 = 87 - 65 = 22 \text{ bhp or } 16 \text{ kW}. \quad (5.7)$$

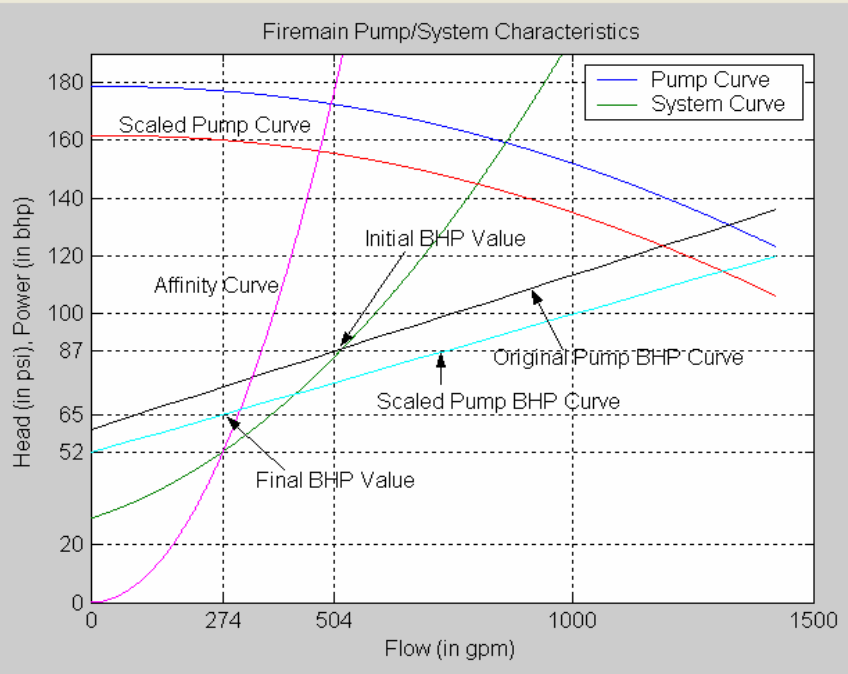

Figure 37. Energy Savings with ASD Implementation on Fire Pump [After Ref. 4.].

Applying the same methodology, the power savings in the chilled water system can be calculated. Use of an ASD in the chilled water system will allow for electrical load savings based on reduced need for unloading flow within the system. Figure 38 below shows the basic Pump/System characteristics for the chilled water system (from Ref. 4).

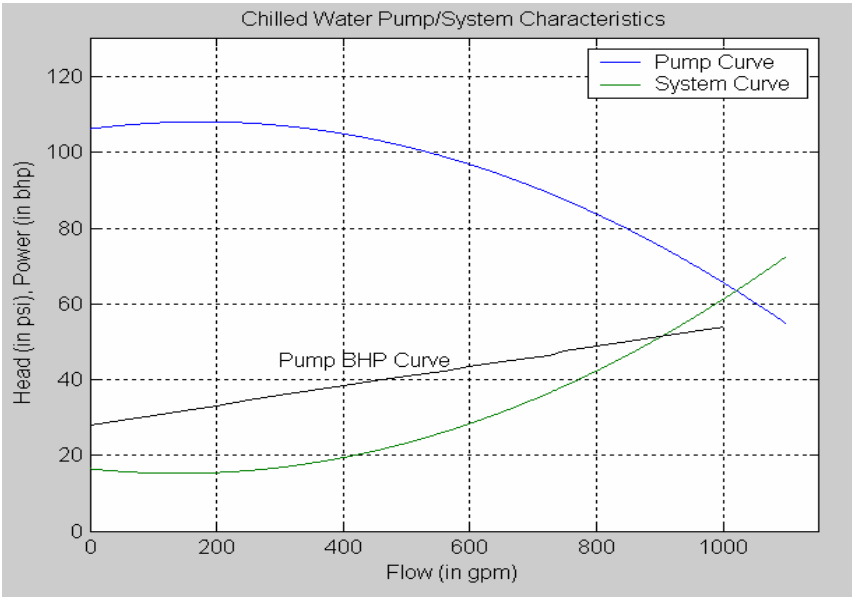

Figure 38. Chilled water system characteristics [After Ref. 4].

Nominal chilled water pump flow can be estimated at 805 gpm with a head pressure of 84 psi. (The unloading valve accounts for 272 gpm.) A final flow, Q_2, of 600 gpm is desired. Minimum final head pressure, H_2, of 28 psi would be needed.

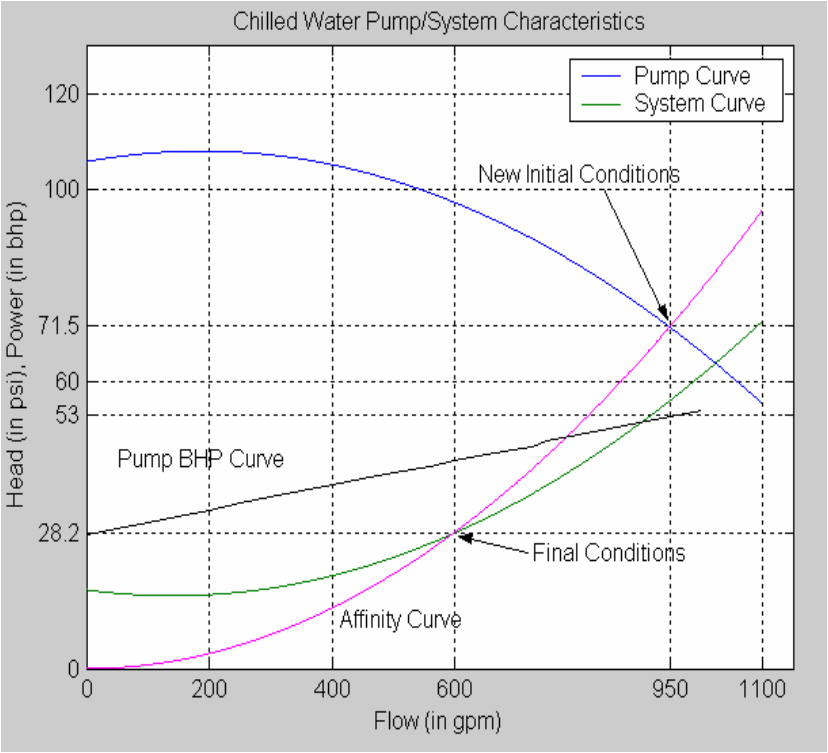

Figure 39. Chilled Water System with Affinity Curve and New Initial Conditions [After Ref. 4.].

In Figure 39:

- The Pump, System, and Pump BHP Curve are from Ref. 4;
- The desired flow, Q_2, is determined by entering the horizontal axis at that value;
- The needed head pressure is identified by moving up vertically to the system curve and see what does that point correspond to along the vertical axis;
- Eq. (5.5) is then used to plot the affinity curve as shown in Figure 39.

The intersection of the affinity curve and the pump curve gives new initial conditions of H_1 equal to 72 psi and Q_1 equal to 950 gpm. Moving vertically down to the Pump BHP curve leads to an initial brake horsepower, BHP_1, of 53 bhp. Using Eq. (5.6), BHP_2 equals 14 bhp. Again, in order to ensure a proper system pressure of 50 psi is maintained

additional input power is required. The pump and BHP curves were scaled by $\left(Q_2^2/Q_1^2\right)$ to produce the scaled curves in Figure 40. The scaled pump curve is based on a pump discharge pressure of 54 psi. (54 psi was chosen to ensure that the required system pressure of 50 psi is maintained.) Moving down vertically from a pump head pressure of 54 psi to the Scaled BHP curve the required brake horsepower, BHP_2, is 17 bhp. Using Eq. (5.7) an overall savings of 36 bhp or 27 kW is achieved for the chilled water system.

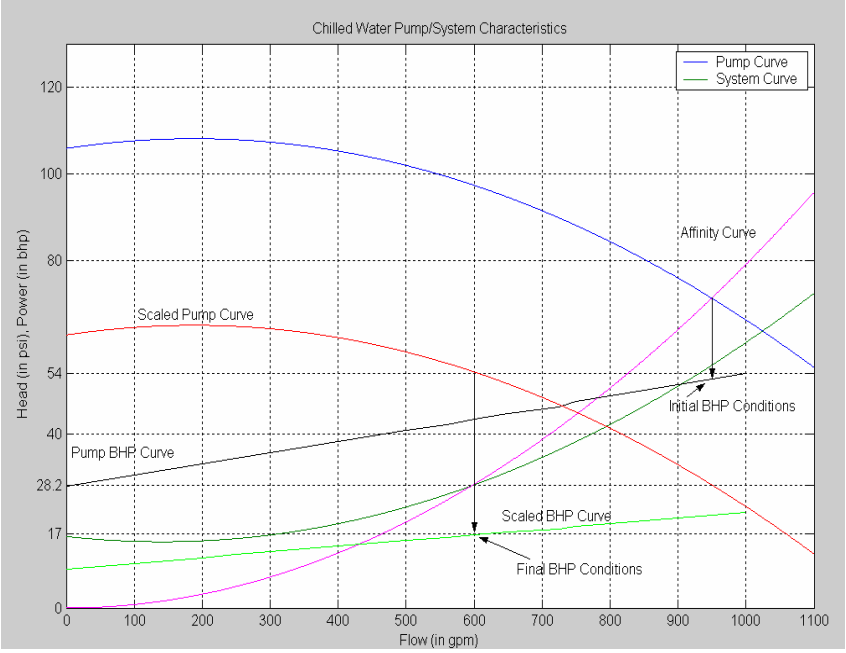

Figure 40. Energy Savings with ASD Implementation on Chilled Water Pump

The total possible savings that can be achieved from these two systems equals 59 bhp or 44 kW operating at normal underway cruise conditions. There is even greater potential for power savings with systems that are only concerned with desired flow at needed head pressure.

The total power required, P_{req} , with these new savings in power consumption is

$$P_{req} = \frac{BHP_{required}}{\eta_{motor/converter}}, \tag{5.8}$$

where $BHP_{required}$ is the total power required to maintain the systems parameters with ASDs and $\eta_{motor/converter}$ is the efficiency of the motor and converter.

There are adaptive control strategies that optimize ASD efficiency, thereby minimizing losses. They quickly find the optimal operating point at any speed and at any load within the operating area with minimal sensors. Three of these control strategies are Simple State Control, Model Based Control, and Search Control. [27]

In simple state control one parameter is measured or derived from measurements and used as feedback in a control loop to track it to its reference. Normally rotor slip frequency, f_{slip}, or displacement power factor, DPF, is used. Speed information is a requisite for f_{slip} control. DPF control requires measurement of the motor active input power and apparent power or the phase shift between the stator voltage and current [27].

Model-based control employs a model of the motor and sometimes the converter. The plant response is forced to follow the response of the reference model regardless of the actual plant parameter variation. The model has fixed parameters that are stored in the processor; therefore, the plant response is insensitive to the parameter variation. Optimizing the efficiency reduces the flux at low-load conditions. Again the price paid for energy savings is a lower stall torque [27].

Search control requires that the active input power is measured somewhere in the system and then the active power is minimized by stepping one of the drive variables: slip frequency, magnetizing current or stator voltage [28].

Maximum Torque per Ampere (MTA) provides a different control strategy. MTA minimizes the stator current amplitude for a given load torque. The motor efficiency achieved with MTA is pretty close to optimal and it is insensitive to changes in rotor resistance. MTA torque response is not as fast as for vector control strategies, but it is still very fast. The slip speed based on motor synchronous reference frame dynamic equations is calculated in order to ensure that maximum efficiency is maintained. This relationship is governed by

$$\omega_{s,ME} = \sqrt{\frac{r_r^2 r_s \omega_b^2}{r_r X_m^2 + r_s X_{rr}^2}} \tag{5.9}$$

where $\omega_{s,ME}$ is the maximum efficiency slip speed, r_r is the rotor resistance, r_s is the stator resistance, ω_b is the base electrical angular velocity, X_m is the magnetic reactance, and X_{rr} is the self-reactance of the rotor [28]. Then the efficiency can be found using,

$$\eta = \frac{X_m^2 r_r \omega_r \omega_s}{r_r^2 r_s \omega_b^2 + X_m^2 r_r \omega_s^2 + X_{rr}^2 r_s \omega_s^2 + X_m^2 r_r \omega_r \omega_s} \tag{5.10}$$

where η is the motor efficiency, ω_r is the electrical rotor speed, and ω_s is the slip speed. The electrical rotor speed ω_r is

$$\omega_r = \frac{P\omega_{rm}}{2} \tag{5.11}$$

where ω_{rm} is the mechanical speed of the motor in radians per second found by

$$\omega_{rm} = \frac{N2\pi}{60} \tag{5.12}$$

with N equal to the speed of the rotor in revolutions per minute, rpm. A 50-hp AC induction motor has the following parameters: $X_m = 13.08\ \Omega$, $r_r = 0.228\ \Omega$, $r_s = 0.087\,\Omega$, $X_{rr} = 0.0302\ \Omega$, $\omega_b = 377$ rad/s, and $\omega_r = 366.52$ rad/s. The slip speed for max efficiency, $\omega_{s,ME}$, equals 4.06 rad/s, and achieves an efficiency of 98%. The efficiency for a 150-hp motor, which was the largest motor studied, would likely have a comparable efficiency value of 94–95%. The additional losses are the result of core losses. The new power requirements for the systems can be calculated using Eq. (5.8). The power required for the firemain and chilled water systems would equal

$$P_{req} = \frac{BHP_{required}}{\eta_{motor/converter}} = \frac{82\text{ bhp}}{0.95} = 86.32\text{ bhp} \times 746 = 64.37\text{ kW}. \tag{5.13}$$

This represents a 38% reduction of input power required to operate the two pumps.

D. POTENTIAL FUEL SAVINGS

An Arleigh Burke destroyer operational cycle typically consists of underway-training exercises and one six-month deployment over a 24-month period. A deployed destroyer averages 23 days underway and when in a non-deployed status, it averages 9

days underway [29]. The destroyer spends approximately 85% of its time underway in cruise steaming conditions. At cruise conditions the average nominal load on the Ship Service Turbine Generators (SSTG) is 3 MW [29]. At this rate of power consumption, the amount of fuel consumed by the SSTGs can be determined via,

$$Fuel_{gallons} = \frac{sfc \cdot pwr \cdot time}{(8.33 \cdot 746)}, \tag{5.14}$$

where *sfc* is the specific fuel consumption (in lbs/hp-hr), *pwr* is the electrical load on the SSTG (in watts), and *time* is the period it is operating at that level (in hours). The constants 8.33 and 748 are the conversion factors to convert from pounds to gallons and horsepower to watts, respectively. The *sfc* is taken from Figure 41 [31].

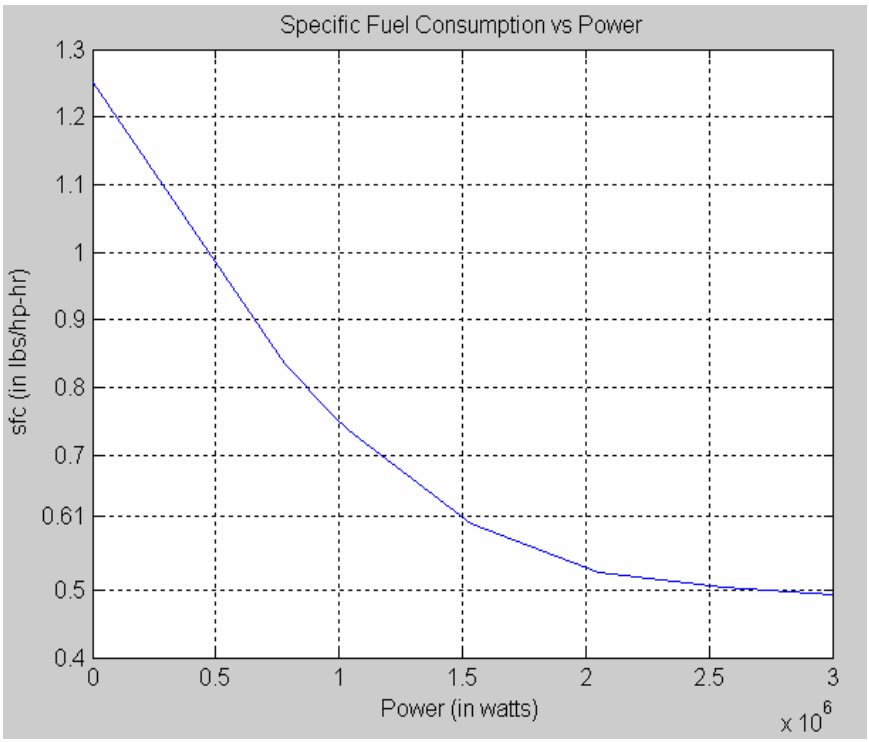

Figure 41. Specific Fuel Consumption vs Power

With a 1.5 MW load on a SSTG , the *sfc* is 0.61 lb/hp-hr and *time* is approximately 20 hrs/day . The fuel consumed during that period equals 2944 gallons. The fuel consumed with the implementation of ASDs on a firemain and chilled water pump would equal 2913 gallons. This is due to the new *sfc* associated with the reduced

required power values. A *sfc* of 0.62 lb/hp-hr and power of 1.46 MW is shown on Figure 42. The reduction is the 39.67kW from the power savings calculated in Chapter V, Section C.

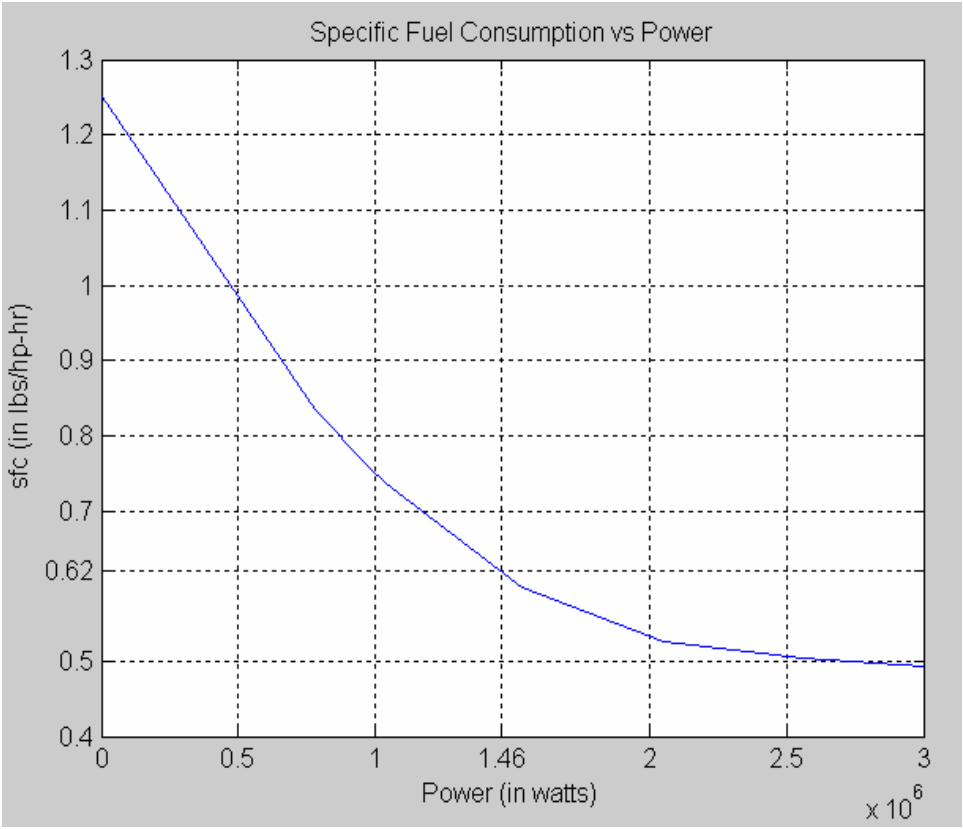

Figure 42. Specific Fuel Consumption vs Power with ASDs

Over a 6-month deployment with fuel cost of $1.29 per gallon, an Arleigh Burke destroyer could potentially save $5674 in reduced fuel consumption [30]. Considering the 18 months of exercises and training that takes place prior to deployment in which an Arleigh Burke destroyer averages 9 days underway, the potential fuel-cost savings would total $6479. That equates to a potential saving of approximately $12,000, which is 1% of the fuel cost without the ASD installations. As more systems and motors are equipped with ASDs, the potential for an increase in fuel-cost savings is significant. Table 10 illustrates the savings that may be achieved.

	Fuel (gallons)	Cost	Days Underway	Total Fuel Cost	Fuel Savings
Underway (Deployed Status)	2944	$1.29	138	$524,247	
Underway (Deployed Status w/ ASD)	2913	$1.29	138	$518,572	$5674
Underway (Non-deployed status)	2944	$1.29	162	$615,237	
Underway (Non-deployed status w/ASD)	2913	$1.29	162	$608,758	$6479

Table 10. Fuel Cost Savings over 24 a Month Training and Deployment Cycle.

The estimated cost for the purchase and installation of the ASDs on the candidate pumps is approximately $50,000 [4]. Disregarding fuel price fluctuations, it would take 7-8 years to recover the cost of the investment. It would have to be determined whether 7-8 year payback period is acceptable to the department of the Navy over the life of a ship. Table 11 below shows the savings accrued over a 40-year ship lifecycle.

		Future value at 2.75% interest rate (over 40 years)	Future value at 1.75% interest rate (over 40 years)	Future value at .75% interest rate (over 40 years)
Fuel Savings/year	$6,000	$427,608	$343,405	$278,679
Initial Investment	$50,000	$147,994	$100,080	$67,417
Differential		$279,615	$243,325	$211,262
Savings/year (over 40 year period)		$6,754	$6,083	$5,282

Table 11. Projected Savings over a 40-Year Ship Lifecycle.

E. CHAPTER SUMMARY

Chapter V introduced the candidate systems chosen for this study and explained their operational parameters. The concept of an affinity curve was introduced. Using the affinity curve and manipulation of the affinity formula's power savings were calculated. Adaptive control techniques for optimum efficiency of the drives were examined. In

closing potential fuel cost savings were determined and the time to realize a return on investment estimated. Chapter VI will summarize the results of this study.

VI. CONCLUSION

A. PURPOSE

The purpose of this thesis was to develop an analysis strategy to quantify the operational cost savings of ASD implementation on Arleigh Burke destroyers. There are very few publications available for navy-specific applications of ASDs.

B. THESIS OVERVIEW

The elements of an ASD were identified and their theory of operation was explained. Some of the technical challenges, which must be addressed in order for successful implementation, were discussed and possible solutions were explored. The inefficiency of conventional throttled-flow was reviewed. The final chapter provided the results of an analysis of the potential power savings with an ASD installed on firemain and chilled water pump systems. The total power saved was then used in calculating fuel cost savings. Over a two-year training and deployment period a potential savings of $12,000 in fuel expenditures was determined. That equates to an approximate 1% saving over the current fuel cost. It was determined that an estimated 7-8 years would be needed to payback the $50,000 investment for the ASDs. Additional potential applications of ASDs aboard ship have been identified in Table 7 and Table 1. If ASDs were installed on these systems, even greater savings could be realized.

C. FUTURE WORK

The Navy has decided that the next generation of destroyers, DD(x), will rely on electric propulsion and will incorporate an IPS. The basic principle of an IPS is that the same generators can be used to provide power for propulsion and ship services via a power conversion module. The result will be a reduced number of installed prime movers and their associated equipment. This will unlock propulsion power for other uses (e.g., Rail Guns and Free Electron Lasers) and help reduce fuel, maintenance, and manning costs throughout a ship's lifecycle. IPS will possibly incorporate ASD technology because of the following benefits:

- There is less wear on the motor and the flow system;
- There are reduced maintenance requirements;
- The pump system becomes more efficient;
- Obtaining a nearly unity power factor.

The benefits will have to be weighted against the hurdles facing the installation of ASDs on the DD(x) class or Arleigh Burke destroyers. Solutions must be developed:

- So as to accommodate the size and weight of ASDs and their peripheral equipment;
- In order to counter the possible damage to electrical cables insulation caused by high *dv/dt*;
- In order to ensure that the motors do not overheat from input harmonics or operation at different speeds;
- So as to minimize damage to motor bearings from bearing currents;
- In order to reduce the high cost of ASDs and their peripheral equipment.

Careful evaluation of these factors will determine whether the U.S. Navy should invest in ASDs for its fleet. If a decision to invest in ASDs is made, the methodology used in this study could be used to determine the projected fuel cost of these ships.

This thesis only looked at two pumps out of a possible 34 candidates. Further analysis of the remaining pumps/motors is recommended in order for a more complete analysis of potential power savings. The Power Electronics Program at the Naval Post-graduate School (NPS) provides a good background on the theory of electric machines. An ASD test lab could be established at NPS so the different control methods mentioned in this study could be further explored. Also a test bed could be constructed to test the accuracy of the proposed pump flows and the required input power.

APPENDIX: MATLAB CODE

The affinity curve MATLAB script file that was used to produce the affinity curve for analysis purposes is provided below. The next MATLAB script file was used to make specific fuel consumption predictions so that fuel savings could be calculated.

```
clc
% recreating the Pump and System curves %
x = [ 0 75 150 225 300 375 450 525 600 675 750 825 900 975 1050 1125 1200 1275
1350 1425] % range of flow in gpm
y = [178 177.8 177.6 177.5 177 176.5 175 173 171.5 168 164 160 157 152 147 144 140
134 129 125]% range of Head in psi
t = 2
p = polyfit(x,y,t)
xi = linspace(0,1425,1400);
yp = polyval(p,xi);
xs = [ 0 75 150 225 300 375 450 525 600 675 750 825 900 975 1050 1125 1200 1275
1350 1425]  % range of flow in gpm
y1= [38 40 42 45 50 55 67 80 95 115 134 152 172 202 222 242 262 282 302 322]
% range of Head in psi
ps = polyfit(xs,y1,t)
ys = polyval(ps,xi);
plot(xi,yp,xi,ys)
legend('Pump Curve','System Curve')
grid on;
axis([0 1500 0 190]);
ylabel('Head (in psi), Power (in bhp)  ')
xlabel('Flow (in gpm)')
title('Firemain Pump/System Characteristics')
hold on
BHPorig = linspace(60,136,20);
plot(x,BHPorig,'k-')
% Scaled Pump curve %
yprime = [161 160.8 160.6 160.5 160 159.5 158 156 154.5 151 147 143 140 135 130 127
123 117 112 108]; % range of Head in psi
t = 2
psc = polyfit(x,yprime,t)
xi = linspace(0,1425,1400);
ypsc = polyval(psc,xi);
plot(xi,ypsc);
grid on;
axis([0 1500 0 190]);
plot(xi,ypsc,'r-');
% Affinity Curve %
```

```
H2 = 52; % Final Head value in psi
Q2 = 274; % Final Flow in gpm
Q1 = (0:1:1500);
z = ((Q1./Q2).^2);
H1 = z* H2;
plot(Q1,H1,'m-')
text(130,110,'Affinity Curve')
BHPscal = linspace(52,120,20);
plot(x,BHPscal,'c-')
% calculating the Brake HP savings %
q1 = 500;
q2 = 274;
bhp1 = 87;
bhp2 = bhp1*(q2./q1).^3
% recreating the Pump and System curves for chilled Water System%
figure(5)
x = [ 0 50 100 150 200 250 300 350 400 450 500 560 600 650 725 750 800 850 900 950
1000] % range of flow in gpm
y = [107.5 107.7 107.9 107.7 107.5 107 106 105 104 103 102 99.7 98 95 93 90 87.5 79
75 69 66]% range of Head in psi
t = 2
p = polyfit(x,y,t)
xi = linspace(0,1100,1400);
yp = polyval(p,xi);
xs = [ 0 50 100 150 200 250 300 350 400 450 500 560 600 650 725 750 800 850 900 950
1000]  % range of flow in gpm
y1= [13.6 14 15 16 17 18 19 20 21 22 23 27.4 28 30 32.5 35 40 45 50 58 66]          %
range of Head in psi
ps = polyfit(xs,y1,t)
ys = polyval(ps,xi);
plot(xi,yp,xi,ys);
legend('Pump Curve','System Curve')
grid on;
axis([0 1150 0 130]);
ylabel('Head (in psi), Power (in bhp)')
xlabel('Flow (in gpm)')
title('Chilled Water Pump/System Characteristics')
hold on
BHPorig = linspace(60,136,20);
plot(x,BHPorig,'k-')
% Affinity curve  %
H2 = 28.5;          % Final Head value in psi
Q2 = 600;           % Final Flow in gpm
Q1 = (0:1:1100);
z = ((Q1./Q2).^2);
H1 = z* H2
```

```
plot(Q1,H1,'m-')
text(130,30,'Affinity Curve')
% recreating Pump BHP curves
BHPorig = linspace(28,54,21);
plot(x,BHPorig,'k-')
text(700,40,'Pump BHP Curve')
 % Scaled Pump curve %
scaled = y-43
t = 2
psc = polyfit(x,scaled,t)
xi = linspace(0,1100,1400);
ypsc = polyval(psc,xi);
plot(xi,ypsc);
grid on;
axis([0 1100 0 130]);
plot(xi,ypsc,'r-');
BHP1scal = linspace(9,22,21);
plot(x,BHP1scal,'g-')
**************************************************************************
%calculating the specific fuel consumption savings
% clc
% DD501 SSTG Data
p = 4
DDA501_gen_load = [0.0 0.282 0.355 0.379 0.564 0.759 0.947 1.00];
DDA501_gen_eff = [0.823 0.9456 0.9544 0.9564 0.9653 0.9693 0.9701 0.9701];
PWR = (DDA501_gen_load*3e6)/746
NPWR = (PWR - mean(PWR))./std(PWR)
S = polyfit(NPWR,DDA501_gen_eff,p)
Y = polyval(S,NPWR)
plot(PWR,Y)
grid on;
figure(2)
DDA501_gen_load1 = [0.0 0.261 0.326 0.347 0.511 0.685 0.854 1.00];
DDA501_gen_sfc = [1.25 0.8510 0.7494 0.7243 0.6006 0.5345 0.4958 0.4958];
PWR1 = (DDA501_gen_load1*3e6)
NPWR1 = (PWR1 - mean(PWR1))./std(PWR1)
S1 = polyfit(NPWR1,DDA501_gen_sfc,p)
Y1 = polyval(S1,NPWR1)
plot(PWR1,Y1)
grid on;
ylabel('sfc (in lbs/hp-hr)')
xlabel('Power (in watts)')
title('Specific Fuel Consumption vs Power')
%LM2500 data
figure(3)
khp = [1.8 2.35 3.125 4.5 5.7 7.75 9.0 11.0 14.5 17.2 21.4 23.9 27.0]*1E3
```

```
pwr = khp*746
sfc = [1.5 1.2 1.0 0.8 0.7 0.6 0.55 0.50 0.45 0.425 0.4 0.39 0.38];
sfc2 = 1.0./sfc;
npwr = (pwr - mean(pwr))./std(pwr)
[c] = polyfit(npwr,sfc2,p)
y = 1.0./polyval(c,npwr)
plot(pwr,y)
grid on;
```

LIST OF REFERENCES

[1] Richard Okrasa, "Adjustable Speed Drive- Reference Guide," eds., pp. 11–109, Ontario Hydro, Canada, August 1997.

[2] "Efficiency Opportunities with Adjustable Speed Drives," pp. 1–3, Pacific Gas and Electric, May 1997.

[3] APOGEE Interactive Inc., "Motors and Drives-Initial Cost," found at http://cipco.apogee.net/mnd/mdadini.asp. Last Accessed on 12 August 2003.

[4] Arthur E Dresser, "Integrated Power System Variable Speed Drive Applications Study," pp. 1–74, Bath Iron Works, Bath, Maine, December 1999

[5] Scott Fausneaucht, "VSD Spells Savings: Variable Speed Drives-a Cost-Effective Option," pp.1–3, *Auto Laundry News*, New Jersey, August 2002.

[6] "Tesla's Induction Motor," found at http://www.ee.umd.edu/~taylor/tesla.htm. Last accessed on 12 August 2003.

[7] Mauri Peltola "Slip of AC Induction Motors and How to Minimize It," ABB Oy, Drives found at http://www.ieee-kc.org/library/motors/motorslip.htm. Last accessed on 11 Aug 2003.

[8] N. Mohan, T. Underland and W. Robins, *Power Electronics: Converters, Applications and Design*, 2nd edition, pp. 400–438 and 626-638, John Wiley and Sons, New York, 1995.

[9] Raymond Ramshaw and R.G. van Heeswijk, *Energy Conversion: Electric Motors and Generators,* pp. 255–265, Saunders College Publishing, Philadelphia, 1990.

[10] Stephen J. Chapman, *Electric Machinery Fundamentals*, pp. 339–379 and pp. 482–504, McGraw Hill, New York, 1985.

[11] Bimal K. Bose, *Power Electronics and Variable Frequency Drives,* pp. 210–217, IEEE Press, New York, 1997.

[12] Geoff Brown, "Harmonics Problem? Then Get Active!," ABB Motors and Drives, Supplement February 2002, found at http://www.dpaoonthenet.net/drives/drives_feb0201.htm. Last accessed on 13 August 2003

[13] Mark Ziemer, "The B-A-S-I-C-S of VSD's," Business News Publishing 2003, found at http://www.esmagazine.com/CDA/ArticleInformation/features/BNP__Features__Item/0,2503,65070,00.html. Last accessed on 12 August 2003.

[14] Bimal K. Bose, *Power Electronics and AC Drives*, pp 232–291, Prentice-Hall, New Jersey, 1986.

[15] Square D Company, "Power System Harmonic-Causes and Effects of Variable Frequency Drives Relative to the IEEE 519–1992 Standard," Product Data Bulletin, Bulletin number 8803PD9402, August 1994.

[16] Pacific Gas and Electric Company, "Power System Harmonics," pp 1–5, found at http://www.pge.com/002_biz_svc/002c1i_power_sys.shtml. Last accessed on 15 August 2003.

[17] Annette von Jouanne and Prasad N. Enjeti, "Design considerations for an inverter output filter to mitigate the effects of long motor leads in ASD applications," *IEEE Trans. on Industry Applications*, pp. 1138–1142, Vol. 33, No. 5, September/October 1997

[18] Annette von Jouanne and Haoran Zhang, "Suppressing common-mode conducted emi generated by pwm drive systems using a dual-bridge inverter," Applied Power Electronics Conference and Exposition, pp.1017–1020, 1998. Volume: 2, February 1998.

[19] Dave Busse, Jay Erdman, Russ Kerkman, Dave Schlegel, and Gary Skibinski, "Characteristics of shaft voltages and bearing currents," *IEEE Trans. Industry Applications Magazine*, pp. 21–32, November/December 1997

[20] Rockwell Automation, "Inverter-Driven Induction Motors Shaft and Bearing Current Solutions," pp. 3–11 and 17–24, White Paper, 11 March 2002.

[21] Reliance Electric," Considerations for the Use of AC Induction Motors on Variable Frequency Controllers in High Performance Applications," found at http://www.reliance.com/prodserv/motgen/b7093.htm. Last accessed on 20 August 2003

[22] Allen Bradley, "Energy savings with adjustable frequency drives," pp. 2-11, Rockwell Automation, August 2001

[23] EPRI PEAC Corporation, "Potential Energy Savings with ASD Control," found at http://www.epri-peac.com/tutorials/brf47tut.html. Last accessed on 20 August 2003.

[24] Ron Carlson, "The correct method of calculating energy savings to justify Adjustable-frequency drives on pumps," *IEEE Trans. on Industry Applications*, Vol. 36, No. 6, pp. 1725–1733, November/December 2000.

[25] "Variable-Speed Integral Motor Pump Technology Support," pp. 3–5, AMSEC LLC, Arlington, VA, January 2001

[26] "DDG-51 Class Chilled Water Systems Training Aid Manual," pp. 1-25, Naval Business Center, Pennsylvania, April 1999

[27] F. Abrahamsen, J.K. Pedersen, and F. Blaaberg, "State-Of-The-Art of optimal efficiency control of low cost induction motor drives," Proceed. of PEMC 1996, Vol. 2, pp. 163–170, 1996.

[28] O. Wasynczuk, S. D. Sudhoff, K. A. Corzine, Jerry L. Tichenor, P. C. Krause, I. G. Hansen, and L. M. Taylor, "A maximum torque per ampere control strategy for induction motor drives," *IEEE Trans. On Energy Conversion*," Vol. 13, No. 2, pp. 163–168, June 1999.

[29] LCDR R. Taylor in a private phone conversation, 08 September 2003

[30] Amory Lovins and Chris Lotspeich, "Energy Efficiency Survey Aboard USS Princeton CG-59," Rocky Mountain Institute, March 2001.

[31] John Ciezki in a private phone conversation, 05 September 2003

THIS PAGE INTENTIONALLY LEFT BLANK

INITIAL DISTRIBUTION LIST

1. Defense Technical Information Center
   Ft. Belvoir, Virginia

2. Dudley Knox Library
   Naval Postgraduate School
   Monterey, California

3. John P. Powers
   Chair, Department of Electrical and Computer Engineering
   Naval Postgraduate School
   Monterey, California

4. Robert W. Ashton
   Department of Electrical and Computer Engineering
   Naval Postgraduate School
   Monterey, California

5. John Ciezki
   Department of Electrical and Computer Engineering
   United States Naval Academy
   Annapolis, Maryland

6. Andrew A. Parker
   Department of Electrical and Computer Engineering
   Naval Postgraduate School
   Monterey, California

7. Godfrey D. Weekes
   Indianapolis, Indiana